Excitation of isomeric states in photonuclear reactions

Yu. P. Gangrskiĭ and A. P. Tonchev
Joint Institute for Nuclear Research, Dubna

N. P. Balabanov
P. Khilendarsky University, Plovdiv, Bulgaria

Fiz. Élem. Chastits At. Yadra **27**, 1043–1098 (July–August 1996)

The experimental data on the probabilities of exciting isomeric states in (γ,γ') and (γ,n) photonuclear reactions at energies from threshold to the giant dipole resonance are reviewed. The isomeric ratios for $g_{9/2}$, $h_{11/2}$, and $i_{13/2}$ single-particle neutron states are given, together with those for two-quasiparticle states and shape isomers. The experimental values of the isomeric ratios are compared with the values calculated using the statistical model. The properties of nuclear levels in the energy range 1–6 MeV, via which isomeric states are populated, are discussed. © *1996 American Institute of Physics.* [S1063-7796(96)00504-9]

1. INTRODUCTION

One of the main sources of information about the properties of excited states of nuclei is nuclear reactions involving various bombarding particles. These reactions allow the determination of several parameters of individual levels (spins, parities, electric and magnetic moments, matrix elements of radiative transitions), and give information about the statistical properties of the levels at high excitation energies (the dependence of the level density on energy and angular momentum). Obviously, when various bombarding particles are used, certain subsets of nuclear levels are selected and only some of these parameters are clearly manifested. Therefore, by using a wide range of particles (from γ quanta to heavy ions) to study nuclei, it is possible to obtain a complete picture of the properties of nuclear levels up to high excitation energies.

The main feature of photonuclear reactions (PNRs) is the fact that the interaction between the bombarding particle (a γ quantum) and the nucleus is entirely electromagnetic. Therefore, the nuclear properties related to electric charge are primarily manifested in PNRs. For example, in γ absorption by nuclei an important role is played by electric and magnetic resonances of various multipole orders, which determine the value of the reaction cross section. The main one is the giant dipole resonance arising from the collective motion of the protons relative to the neutrons in the nucleus.

The special feature of γ quanta as compared with other bombarding particles in nuclear reactions is the absence of a binding energy and Coulomb barrier. Consequently, the nuclear excitation energy corresponds to the energy of the absorbed γ, and the reaction cross section is sizable down to very low excitation energies. This gives rise to the unique possibility of studying PNRs and the levels involved in them at low excitation energies below the nucleon binding energy. In addition, at energies $E_\gamma \leqslant 30$ MeV the γ wavelength is noticeably larger than the nuclear size (for example, at $E_\gamma = 15$ MeV and $A = 125$ the values of λ and R are, respectively, 80 F and 6 F). In the long-wavelength approximation the electric dipole absorption of γ quanta dominates, and the contribution of magnetic dipole or electric quadrupole absorption amounts to only a few percent. Therefore, in this energy range the γ contributes to the nucleus an angular momentum close to $1\hbar$, and this value is practically independent of the γ energy. This strongly limits the range of spins of the excited levels and simplifies the interpretation of the results.

Studies of the properties of levels excited in PNRs are focusing on several areas. One is the measurement of the energy or angular distributions of the particles or γ quanta emitted in PNRs. Another is the measurement of both the total and the partial cross sections corresponding to the excitation of certain final states. In the last case the measurements will be more effective if the final state is an isomeric state with sufficiently large half-life, so that the bombardment and measurement processes are well separated in time. By performing the measurements in the absence of the γ beam bombarding the target, it is possible to significantly lower the background and raise the sensitivity of the experiments, so that levels excited in reactions with cross sections of as little as a fraction of a microbarn can be studied.

At the present time, more than a hundred isomeric excited states with half-life greater than 1 sec are known.[1] The main reason for the existence of isomers is a large difference between the spins of the isomeric and ground states of nuclei ($\Delta I \geqslant 3$). Such isomers are concentrated in regions of nuclei with the number of protons or neutrons just less than that of a filled shell (50, 82, or 126). In deformed nuclei there is a selection rule in the quantum number K (the spin projection on the nuclear symmetry axis). It greatly retards radiative transitions of small multipole order, thus leading to the appearance of isomers. In heavy nuclei of the actinide elements (from U to Bk) there are excited states characterized by quadrupole deformation significantly larger than for the ground state (shape isomers or spontaneously fissioning isomers[2]). The large difference between the deformation parameters also causes radiative transitions to be strongly forbidden. However, the probability for spontaneous fission from an isomeric state is strongly increased, so that the lifetimes of such nuclei turn out to be small ($< 10^{-2}$ sec).

An isomeric state is usually associated with an entire set of levels lying above it and having the same structure: a rotational or vibrational band constructed on the isomer, the components of a single multiplet with the same number of

 1063-7796/96/040428-25$10.00

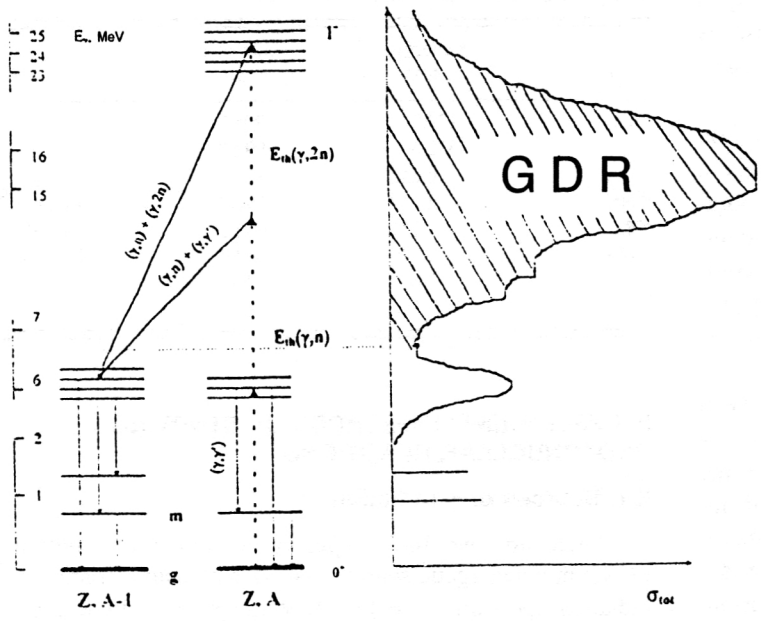

FIG. 1. Scheme of isomer excitation in photonuclear reactions.

quasiparticles. Radiative transitions between the levels of this system are usually more probable than those to other levels. The study of these levels and measurement of their parameters is very interesting because it allows the isomer structure to be understood in more detail. For example, by studying the properties of the levels associated with shape isomers, it has proved possible to obtain complete information about the structure of the potential barrier in heavy nuclei: the depth of the potential well, the heights of the inner and outer barriers, and the nuclear deformation in the isomeric state.

However, the study of the properties of such states presents certain difficulties. These states are usually not manifested in β decay, and in nuclear reactions involving charged particles or neutrons they cannot always be isolated from the other excited levels. However, the features of PNRs mentioned above make these reactions useful for studying such levels.

The set of excited states involved in isomer population is largely determined by the type of PNR used and the energy of the γ radiation. When bremsstrahlung radiation with a continuous energy distribution (from zero to the maximum value) is used in γ capture, it is possible in principle to excite all the levels connected to the ground state by radiative transitions which are allowed by the spin and parity selection rules. However, actually only those levels with large reduced probabilities of radiative transitions to the ground state are excited, and transitions of low multipole order dominate. These levels usually belong to collective multipole resonances or have large admixtures of such resonances in their wave function. Among them the strongest is the above-mentioned giant dipole resonance lying in the range 15–20 MeV. The main properties of this resonance are discussed in Refs. 3 and 4.

Owing to their very small width, isomeric levels (for $T_{1/2}>1$ sec, $\Delta E<10^{-14}$ eV) are rarely excited in the capture of a γ quantum of energy equal to the energy of the isomeric state; instead, they are populated in radiative transitions from higher levels. These can be both activation levels [in (γ,γ') reactions] and levels populated after the evaporation of a neutron or charged particle from the compound nucleus. When the spins of these levels and the isomeric state differ greatly, a cascade of several γ quanta leads to the latter. The scheme of isomer population in this reaction mechanism is shown in Fig. 1. By measuring the dependence of the isomer population probability on the excitation energy, it is possible to judge which levels participate in this population and to find the values of some of their parameters: the spins and parities, the matrix elements of the transitions to the isomer, and their statistical characteristics. Information about the properties of these levels is usually obtained by comparing the measured probabilities for isomer production with the results of a theoretical calculation based on the method proposed in Ref. 5. Here various level schemes are used in the calculations, and a final choice is made on the basis of which one gives the best agreement with experiment.

It is well known that, in addition to this mechanism of populating an isomeric state, there is a significant probability for another mechanism, in which neutrons or charged particles are emitted until thermal equilibrium is established in the nucleus. These are either direct processes, when a particle is directly knocked out of a nucleus by a γ quantum, or semidirect processes, in which particles are emitted from states formed while thermal equilibrium is being reached. In these processes the probability for populating the individual levels of the final nucleus depends on their spectroscopic factors, which are usually determined from neutron or proton stripping reactions. Here the distribution of the final nuclei in angular momentum and excitation energy will be different from that in the case of thermal equilibrium, and naturally this also changes the isomer population probability. This probability is usually decreased, because the final nucleus has a lower excitation energy, which leads to a shorter γ cascade populating the isomer. The relative contributions of

the two mechanisms depend on the γ energy and on the type of reaction selected. For example, the second mechanism is more probable in the (γ,p) reaction and at higher γ energies.

The calculated isomeric ratios (IRs) naturally depend on the PNR mechanism selected. It is assumed that in a given range of Z and A (intermediate and heavy nuclei) and bombarding γ energy (below 30 MeV), reactions with compound-nucleus formation and establishment of thermal equilibrium in the nucleus dominate. Direct and semidirect processes give a comparatively small contribution. These assumptions are also used to calculate the IRs.

By now a large amount of experimental data has been obtained on the excitation of isomeric states in various PNRs. In this review we systematize these data for the (γ,γ') and (γ,n) reactions leading to the formation of nuclei in isomeric states of various types: one-particle states, multiparticle states, K isomers, and shape isomers. The isomer excitation probability is analyzed on the basis of current ideas about the PNR mechanism, and the ratios are compared with those calculated using various models. The properties of excited levels via which isomers are populated are discussed.

The data on isomer excitation (experimental or obtained from theoretical calculations) are usually presented in two forms:

1. Isomeric ratios corresponding to the ratios of the cross sections for nucleus production in the isomeric and ground states, σ_m/σ_g,

2. Isomer excitation probabilities equal to the ratio of the cross section for isomer production and the total cross section, σ_m/σ_0.

These two ratios are related as

$$\frac{\sigma_m}{\sigma_0}=\frac{\sigma_m/\sigma_g}{1+\sigma_m/\sigma_g},\quad \frac{\sigma_m}{\sigma_g}=\frac{\sigma_m/\sigma_0}{1-\sigma_m/\sigma_0}. \tag{1}$$

Experimentally, the IRs are determined in those cases where the nuclei in the ground and isomeric states are radioactive, and the values of σ_g and σ_m are measured directly in the same experiment. If the final nucleus is stable in the ground state, it is more convenient to obtain the values of the isomer excitation probability. Here σ_0 is determined in separate experiments or is estimated from empirical regularities.

The special feature of PNRs is the fact that in most cases the measured reaction yields pertain not to a definite excitation energy, but to a range of energies (from threshold to the maximum bremsstrahlung energy). Obtaining the reaction cross sections at certain energies from these data is a fairly complicated procedure (it is described below) which cannot always be carried out. Therefore, in a number of cases the IRs given in this review are ratios of integrated cross sections (integrated over the entire range of the bremsstrahlung spectrum) or ratios of reaction yields. The relations between these forms of IR are discussed in each particular case.

TABLE I. Sources of monochromatic radiation.

Nuclide	γ energy, MeV	Intensity, %	$T_{1/2}$
^{60}Co	1173.2	99.90	5.27 yr
	1332.5	99.98	
^{137}Cs	0.662	85.21	30 yr
^{24}Na	2.754	99.94	15.02 h
^{46}Sc	1.121	99.99	83.81 day
^{56}Mn	0.847	98.90	2.578 h
	1.811	27.20	
	2.113	14.30	

2. EXPERIMENTAL METHODS OF STUDYING PHOTONUCLEAR REACTIONS

2.1. Sources of γ radiation

There are two basic types of γ source for studying PNRs: monoenergetic sources and sources with a continuous radiation spectrum. The first type are sources in which γ emission is the result of natural or artificial radioactivity, or of a nuclear reaction of the form (p,γ) or (n,γ). The second type are electron acelerators, at which bremsstrahlung radiation is obtained with an adjustable value of the maximum energy, reaching tens or hundreds of MeV.

The advantage of monoenergetic sources is that the measured cross section can be uniquely assigned to a certain known excitation energy. However, it must be remembered that monochromatic radiation is accompanied by a significant background of γ quanta of lower energy arising as a result of the scattering of the primary radiation on the shielding surrounding the source. In some cases it is actually this low-energy scattered radiation which leads to the excitation of isomeric states.

In Table I we give the characteristics of monochromatic sources: the γ energy, the half-life, and the intensity per β-decay event.[1] The intensity of these sources can be very high, up to millions of curies or 10^{18} sec^{-1}. However, for all of them the γ energy, as can be seen from Table I, is lower than the neutron binding energy, and they can be used only for isomer excitation in inelastic γ scattering reactions.

In Table II we give the characteristics of (n,γ) and (p,γ) reactions in which high-energy γ quanta are emitted.[6]

TABLE II. High-energy γ quanta emitted in neutron and proton capture reactions.

Reaction	E_1^* (MeV)	E_2^* (MeV)	p_1/p_2^{**}	σ (10^{-24} cm^2)
^{14}N$(n,\gamma)^{15}$N	10.829	5.269	0.5	0.075(75)
^{35}Cl$(n,\gamma)^{36}$Cl	5.716	2.864	0.86(7)	43.6(4)
	6.978	1.601	0.65(6)	
^{48}Ti$(n,\gamma)^{49}$Ti	4.882	1.499	0.92	7.84(25)
^{52}Cr$(n,\gamma)^{53}$Cr	5.618	2.321	1.0	0.76(6)
^{53}Cr$(n,\gamma)^{54}$Cr	8.884	0.835	0.6	18.2(15)
^{11}B$(p,\gamma)^{12}$C	13.91	4.44	1.0	
^{23}Na$(p,\gamma)^{24}$Mg	11.588	1.368	0.961(3)	
^{27}Al$(p,\gamma)^{28}$Si	10.76	1.78	0.796(10)	

*E_1 and E_2 are the energies of the γ quanta.
**p_1 and p_2 are the emission probabilities.

TABLE III. Basic parameters of beams at electron accelerators.

Type of accelerator	Electron energy: Maximum energy, MeV	Electron energy: Energy resolution, %	Intensity: Average current, μA	Intensity: Number of particles per second	Intensity distribution: Repetition frequency, Hz	Intensity distribution: Pulse duration, μsec
Microtron	30	0.1–0.5	20	10^{14}–10^{15}	20–1000	0.001–3
RM-100[1)]	120	0.1–0.01	1000			
Dynamotron[2)]	10–130	±13	4000	10^{14}		
Betatron	25–340	0.1–0.5	≤1	10^{12}–10^{13}	6–1000	0.1–3
Linear accelerator	25–50000	10–0.3	10–500	10^{16}–10^{17}	50–1000	0.001–3

[1)]Slot microtron, Institute of Nuclear Physics, Moscow State University.
[2)]TU dynamotron, Darmstadt, Germany.

For a number of these reactions the γ energy is higher than the neutron binding energy, but the intensity is small.

The advantage of bremsstrahlung sources is that they can be used to obtain γ radiation of high energy and high intensity, but the spectrum is continuous up to the maximum electron energy. Currently, there are four types of electron accelerator in common use: the dynamotron, the betatron, the microtron, and the linear accelerator. They have been used to obtain most of the experimental data on PNRs in the region of the giant dipole resonance. In Table III we give the basic parameters of these accelerators.

We see from this table that the current electron accelerators have energies covering the entire range needed for studying PNRs, and that their intensities are sufficient for observing isomers produced even with very small cross section (nanobarns). By using different timings of the electron beam, it is possible to carry out measurements both directly in the bremsstrahlung beam (in this case continuously operating accelerators are most suitable), between bremsstrahlung radiation pulses (for isomers with lifetimes in the range 10^{-6}–10^{-1} sec), and a certain time after bombardment (for isomers with $T_{1/2}>1$ sec). This opens up broad possibilities for studying PNRs leading to the excitation of different types of isomer with a wide range of half-lives and production cross sections.

In recent years, many studies of PNRs with the excitation of isomeric states have been carried out at microtrons. The basic scheme is shown in Fig. 2 (Ref. 7). In the microtron, electrons are accelerated by an electric field varying with constant frequency, and in a constant, radially uniform magnetic field they move in circular orbits having a common point of tangency. At this point is a resonator in which a superhigh-frequency field boosts the electrons. In each passage through the resonator in phase with the accelerating field the electrons acquire a certain energy and move to an orbit of larger radius. When they reach the final orbit, they are extracted from the vacuum chamber via a magnetic channel and directed to the target.

The experimental possibilities of the accelerator are primarily determined by the energy and intensity of the beam of accelerated particles. The distinguishing feature of the microtron is the fact that unlike a linear electron accelerator of average beam intensity, it has a small energy spread of 40–50 keV, which is practically independent of the particle energy. This also determines the lower limit of the energy resolution of microtron measurements to determine the dependence of the yield on the energy of the studied PNRs.

2.2. Detectors of radioactive radiation

As a rule, the activation method is used to measure the cross sections of PNRs in which the nuclides produced in the ground and isomeric states have half-life greater than 1 sec. In this method the sample of isotope under study is irradiated and then transferred to a detector of radioactive radiation (by a tube conveyer, manipulator, or by hand), where its radiation spectrum is measured.

In Fig. 3 we show an example of an irradiation scheme for experiments performed in the bremsstrahlung beam of a microtron using the activation method. The accelerated electrons are directed to a bremsstrahlung target (this is usually a water-cooled tungsten disk several millimeters thick), beyond which is an aluminum absorber several centimeters thick. The irradiated samples (the one under study and a standard one) are located right behind the aluminum absorber. The electron beam is monitored by measuring the total charge that it transfers to the bremsstrahlung target, using an electric-charge integrator.

The yields of the PNRs under study are usually determined from the intensity of the γ radiation emitted in the radioactive decay of the reaction products. The energies of the γ lines in the spectrum and the time dependence of their

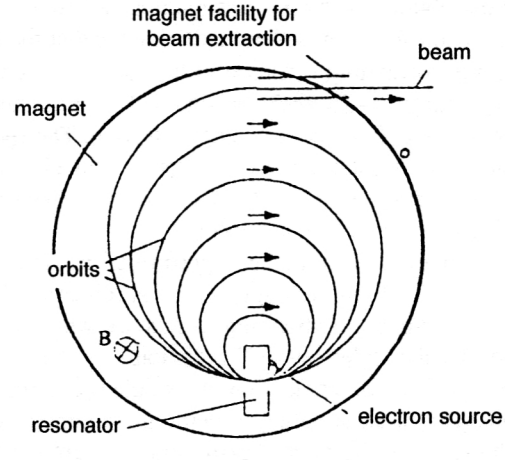

FIG. 2. Basic scheme of electron acceleration in the microtron.

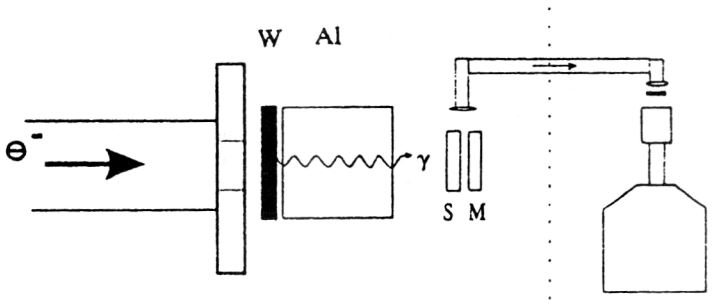

FIG. 3. Bombardment of samples in the bremsstrahlung beam of the microtron.

intensity (determined by the nuclide half-lives) allow the identification and measurement of the yields of isotopes produced in the PNRs. The γ spectra are usually measured using scintillation counters with a NaI(Tl) crystal, semiconductor spectrometers of superpure germanium HpGe, or germanium doped with lithium Ge(Li).[6]

2.3. Bremsstrahlung spectrum of the γ radiation

Despite the development of various methods of obtaining monochromatic photons, bremsstrahlung radiation from thick targets continues to be widely used in photonuclear experiments. For analyzing the results obtained using bremsstrahlung radiation, it is necessary to know the shape of the radiation spectrum for various energies E_0 of the accelerated electrons, the γ emission angles θ, and the thicknesses and materials of the bremsstrahlung target.

The angular distribution of the bremsstrahlung radiation is azimuthally symmetric relative to the direction of motion of the electrons. The angular spread of the radiation depends on several factors, one of which is the relativistic (kinematical) spread. The half-width of the angular distribution in this case can be approximately estimated as mc^2/E_0, where m is the electron mass and c is the speed of light. From this it follows that as the electron energy increases, the bremsstrahlung radiation converges to a smaller and smaller solid angle. However, this spread of the radiation will be observed only for very thin targets with thickness equal to 0.01 radiation lengths. For thick targets the multiple scattering of electrons in the target makes a large contribution to the spread. In addition, the electron beams of accelerators have their own angular spread, which gives an additional contribution to the angular distribution of the bremsstrahlung radiation.

It has been shown in several experiments that the largest yield of bremsstrahlung radiation in the forward direction in the energy range 4–25 MeV is obtained when a target of thickness equal to 0.3 radiation lengths is used. The spectrum of radiation from such a target cannot be considered to be equivalent to the Schiff spectrum commonly used for thin targets;[8] it must be calculated specially.

Such calculations have been performed in Refs. 9 and 10, where a thick bremsstrahlung target is represented as the sum of fairly thin bremsstrahlung targets, for which it can be assumed that the "elementary" radiation spectrum, i.e., the emission spectrum of an electron in a single scattering event, is known. The bremsstrahlung spectra are summed over the entire thickness of the target, taking into account the energy lost to electron absorption and scattering, absorption of radiation in the target material, and the probability of backward emission of photons. The bremsstrahlung spectrum is given by

$$\frac{d^2Y}{dKd\Omega}=\sum_{i=1}^{n}\alpha_i\tau_iN_i\frac{d\sigma}{dK}B_i, \quad 1/(\text{MeV}\cdot\text{sr}). \tag{2.1}$$

Here n is the number of layers in the target; i is the number of a layer; α_i is the coefficient of photon absorption in the target material; $\tau_i(T_e,\alpha_i)$ is the transfer coefficient, i.e., the fraction of electrons reaching the ith layer (in cm^{-2}; T_e is the initial electron energy); N_i is the number of atoms along the electron path after the ith layer (in cm^{-2}); $d\sigma/dK[(T_e)_i,\alpha_i]$ is the elementary (intrinsic) bremsstrahlung spectrum, where $(T_e)_i$ is the electron energy in the ith layer, α_i is the coordinate of the ith layer, and B_i is the number of photons emitted into unit solid angle at 0° from the ith layer.

As an example, in Fig. 4 we show the spectra at various angles calculated in this manner for a tungsten target of thickness 2 mm and electron energy in the range from 10 to 30 MeV (Ref. 10). This figure shows the dependence of the bremsstrahlung radiation intensity on the electron angle and energy. The intensity has a maximum in the forward direction and decreases sharply with increasing angle for all γ energies, this decrease being more noticeable for the high-energy part of the spectrum.

The intensity of the bremsstrahlung radiation decreases in inverse proportion to the squared distance to the bremsstrahlung target, so that the sample is usually located right at the target or several millimeters from it.

It is easier to use the calculated bremsstrahlung radiation spectra if they are represented as an analytic dependence, which is more convenient for solving the inverse problem: reconstructing the PNR cross section from the experimental values of the curves. Therefore, the calculated data[10] have been approximated by a polynomial of fourth degree[11] in the energy range 11–22 MeV or by a dependence with five parameters[12] in the energy range 4–12 MeV. This has made it possible to describe the calculated data with an accuracy of better than 10% in these energy ranges.

When these polynomials are used to analyze the experimental results, it becomes possible to include the effect of the degree of monochromaticity of the electron beam on the shape of the bremsstrahlung spectrum, which is important for reconstructing the nuclear reaction cross sections from the measured yields. This can be done using the expression

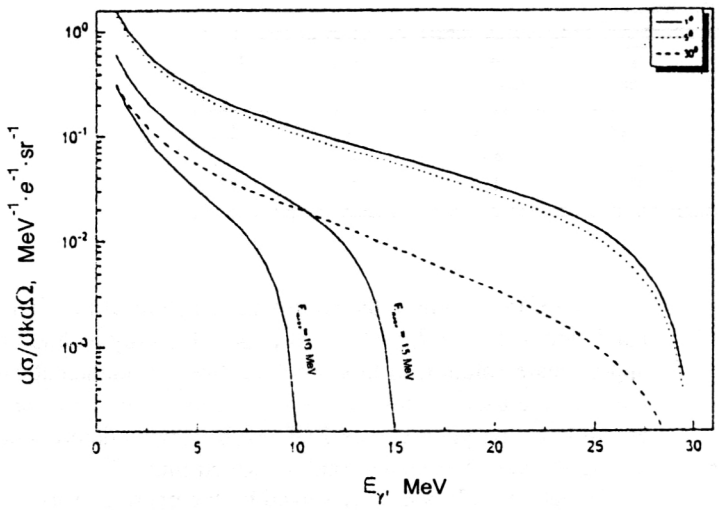

FIG. 4. Calculated shapes of the spectra of bremsstrahlung radiation from thick targets.

$$d^2N/dkd\Omega = \int f_0(\bar{E}_e - E_e) d^2N/dkd\Omega dE_e, \qquad (2.2)$$

where $\bar{E}_e$ is the average energy of the electrons in the beam, and $f(\bar{E}_e - E_e)$ is the shape of the energy distribution of the electrons in the beam, which in the simplest case can be assumed to be a Gaussian.

3. MEASUREMENT OF THE CROSS SECTIONS FOR PHOTONUCLEAR REACTIONS

3.1. Determination of the yields and integrated cross sections

The ultimate goal of this method of measuring the induced activity is to determine the reaction yield, i.e., the number $c(t)$ of nuclei produced during the irradiation time per unit target thickness and γ flux:

$$Y(E_{\gamma\,\max}) = \frac{C(t_i)}{A_0 \int_0^{t_i} \int_{E_{\rm th}}^{E_{\gamma\,\max}} N(E, E_{\gamma\,\max}) dE dt}, \qquad (3.1)$$

where A is the number of nuclei of interest in 1 cm^2 of the target, t_i is the irradiation time, $N(E, E_{\gamma\,\max})$ is the number of γ quanta of energy E in the bremsstrahlung radiation spectrum with maximum energy $E_{\gamma\,\max}$, and $E_{\rm th}$ is the threshold energy of the reaction.

The number of nuclei produced in a reaction is related to the area of the measured γ line in the spectrum of the nuclide in question as

$$c(t_i) = \frac{\lambda S_\gamma}{n_t \varepsilon_\gamma I_\gamma f(t_i, t_d, t_m)}, \qquad (3.2)$$

where S_γ is the area of the photopeak in the γ spectrum, λ is the decay constant, n_t is the number of bombarded nuclei, ε_γ is the γ-detector efficiency, I_γ is the intensity of the γ line in the decay scheme, and $f(t_i, t_d, t_m)$ is the time factor, given by

$$f(t_i, t_d, t_m) = (1 - e^{-\lambda t_i}) e^{-\lambda t_d} (1 - e^{-\lambda t_m}), \qquad (3.3)$$

where t_i, t_d, and t_m are, respectively, the irradiation time, the decay time, and the measurement time.

In the case of a bremsstrahlung spectrum with maximum energy $E_{\gamma\,\max}$, the reaction yield and cross section are related as

$$Y(E_{\gamma\,\max}) = \int_{E_{\rm th}}^{E_{\gamma\,\max}} \sigma_s(E) N(E, E_{\gamma\,\max}) dE, \qquad (3.4)$$

where $\sigma_s(E)$ is the cross section of the studied PNR at γ energy E.

The relative method is often used to find the absolute values of the measured cross sections. Here the yields of the γ line of the studied isotopes or isomers are compared with the yields of the γ line of isotopes whose PNR cross sections are well known from other experiments and taken as standards. Then the object of measurement is the ratio of the yields of the studied nucleus and the standard, bombarded simultaneously in the same geometry. It thereby becomes possible to eliminate the systematic uncertainties introduced in measuring the γ intensity in the absolute method. As the standard in γ inelastic scattering reactions it is convenient to use the reaction ^{115}In$(\gamma,\gamma')^{115m}$In, and, at energies above the nucleon threshold, the reactions ^{65}Cu$(\gamma,n)^{64}$Cu and ^{63}Cu$(\gamma,n)^{62}$Cu. The cross sections for these reactions have been measured many times and are well known.[13–15]

The reactions In(γ,γ') and Cu(γ,n) are widely used as standards, owing to the absence of resonance structure near the threshold energy for these nuclei, the convenient values of their half-lives, the intense γ lines from their decay, the possibility of including the neutron contribution to the measured yields, and the simplicity of the target preparation.

The resulting dependence of the PNR yield on the maximum energy of the bremsstrahlung radiation serves as the basis for determining the reaction cross sections and the excitation function. However, in many cases, especially for small reaction yields, these measurements are possible at only one value of the maximum energy of the bremsstrahlung spectrum. In this case one finds the integrated PNR cross section:

TABLE IV. Monitor reactions used in the activation method.

Reaction	$T_{1/2}$	E_γ keV	I_γ %	σ_{int} MeV·mb	E_{th}	$E_{\gamma max}$
$^{115}In(\gamma,\gamma')^{115m}In$	4.49 h	336.2	45.8	2.8	1.0	10.5
$^{63}Cu(\gamma,n)^{62}Cu$	10 min	511	37.1	496	10.9	23.0
$^{65}Cu(\gamma,n)^{64}Cu$	12.7 h	511	37.1	426	9.9	23.0

$$\sigma_{int}(E_{\gamma\,max})=\int_{E_{th}}^{E_{\gamma\,max}}\sigma(E)dE. \tag{3.5}$$

It is related to the measured yield as

$$Y(E_{\gamma\,max})=\frac{\sigma_{int}(E_{\gamma\,max})}{E_{\gamma\,max}-E_{th}}\int_{E_{th}}^{E_{\gamma\,max}}N(E,E_{\gamma\,max})dE. \tag{3.6}$$

The values of the integrated cross sections for the above standard reactions for different values of $E_{\gamma\,max}$ are given in Table IV.

3.2. Determination of the differential cross sections

If monoenergetic γ sources are used, the PNR cross section can be determined directly. In experiments using bremsstrahlung sources, it is rather difficult to find the cross section, because the bremsstrahlung spectrum must be eliminated from the experimental yield curve. As shown above, the result of measurements in a bremsstrahlung radiation beam is the integrated reaction yield, which is related to the cross section as

$$Y(E)=\sum_i \sigma(E_i)N(E_i,E)dE_i, \quad i=1,\ldots,n, \tag{3.7}$$

where $\sigma(E_i)$ is the effective cross section of the photonuclear reaction under study, $N(E_i,E)$ is the number of photons of energy E_i per unit energy range of the bremsstrahlung spectrum with upper limit E, and n is the number of experimental points.

Equation (3.7) is an integral equation for the unknown effective cross section $\sigma(E_i)$. Therefore, to obtain the effective cross section it is necessary to know the form of the functions $Y(E)$. The experimental values of the yields $Y(E_i)$ are obtained at discrete points corresponding to different values of E_i. Therefore, a system of integral equations of the type (3.7) is usually replaced by a system of linear equations:

$$Y_i=N_{ij}\sigma_j, \quad i=1,\ldots,n, \quad j=1,\ldots,m. \tag{3.8}$$

The matrix of Eq. (3.8) is ill-conditioned. This means that the presence of errors in the experimental data ΔY_i can lead to the appearance of large unphysical oscillations in the desired solution σ_j. The uncertainty in the reaction yield arises from a number of factors:

- the statistical nature of the processes under study;
- the bremsstrahlung radiation source;
- the studied samples and the reproducibility of their location during bombardment and recording of the reaction yield;
- the operating instability of the detection apparatus.

Therefore, owing to the approximate nature of the right-hand side of Eq. (3.7) or (3.8), it is possible only to find an approximate solution to this problem. Special mathematical methods are used for this. They amount to numerical differentiation of the yield curves $Y(E)$ with weights determined by the shape of the bremsstrahlung spectrum.[16–20]

Equation (3.7) is usually solved by the method proposed by Tarasko[21] and later developed by Zhuchko.[22] It is referred to as the method of minimization of the directional discrepancy (MDD), because the measure of the discrepancy between the left- and right-hand sides of Eq. (3.4) is taken to be

$$Y(N,\sigma,J)=\int Y(E_0)\ln\frac{J(E_0)}{\int\sigma(\tilde{E})N(\tilde{E},E_0)d\tilde{E}}dE_0, \tag{3.9}$$

which has the meaning of a directional discrepancy in probability space. The solution of the original equation leads to minimization of the functional (3.9). In this method, *a priori* information about the positivity of the desired function is ensured by choosing the form of the functional (3.9).

In contrast to Ref. 21, where the calculation of $\sigma^{(s+1)}(E_\gamma+\Delta E_\gamma)$ is based on the values of the cross section at the sth step $\sigma^{(s)}(E_\gamma)$, the other method of calculating $\sigma^{(s+1)}(E_\gamma+\Delta E_\gamma)$ uses the values of $\sigma^{(s+1)}(E_\gamma)$ already found for all E_γ in the range $[E_{th},E]$, where $E<E_n$, i.e., for the sth approximation

$$\sigma(E_\gamma)=\begin{cases}\sigma^{(s+1)}(E_\gamma) & \text{if } E_\gamma\leqslant E\\ \sigma^{(s)}(E_\gamma) & \text{if } E_\gamma>E\end{cases}. \tag{3.10}$$

Using the fact that $N^*(E_i,E_\gamma)=0$ for $E_\gamma>E_i$, the iteration process of the MDD method is described by the expression

$$\sigma^{(s+1)}(E_\gamma)=\frac{\sigma^{(s)}(E_\gamma)}{n}\sum_{i=k}^{n}N^*(E_i,E_\gamma)\Bigg/ \times\left[\int_{E_{th}}^{E}\sigma^{(s+1)}(E_\gamma)N^*(E_i,E_\gamma)dE_\gamma+\int_{E_j}^{E_i}\sigma^{(s)}(E_\gamma)N^*(E_i,E_\gamma)dE_\gamma\right], \tag{3.11}$$

where k is such that $E_k\geqslant E_\gamma$, $\sigma^{(1)}(E_\gamma)=\text{const}$, and $N^*(E_1,E_\gamma)$ and $\sigma(E_\gamma)$ are normalized according to (3.5).

This process always converges to a non-negative function satisfying the original equation (3.4). Therefore, the method of directional discrepancy satisfactorily describes the cross sections both in the vicinity of the giant dipole resonance and near the reaction threshold for all experiments using bremsstrahlung radiation.

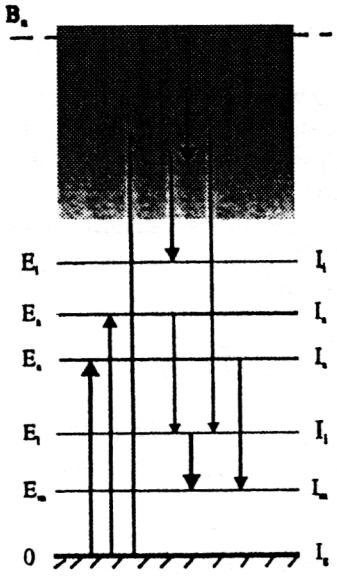

FIG. 5. Isomer excitation in γ inelastic scattering.

4. THE (γ,γ') REACTION WITH ISOMER EXCITATION

Recently, there has been great interest in nuclear excitation below the nucleon threshold in (γ,γ') reactions using γ radiation with an energy of several MeV. This is a consequence of the discovery of low-lying collective magnetic dipole transitions, called the "scissors" mode, in which the proton and neutron deformed ellipsoids rotate with opposite phases about a common axis perpendicular to the nuclear symmetry axis. It is also a consequence of the observation of excessively large values of the reduced probabilities of electric dipole transitions in heavy deformed nuclei. Another area of experimental activity is the resonance excitation of isomers characterized by unusually large cross sections. This phenomenon might have a bearing on the creation of γ lasers based on nuclear transitions, on nuclear astrophysics, and on other new phenomena.

4.1. Resonance excitation of nuclear levels

Isolated states are excited when nuclei are bombarded by monochromatic γ quanta or bremsstrahlung radiation of energy below the nucleon binding energy. These states decay by emitting γ quanta either of the same energy, with the nucleus going to the ground state (elastic channel), or with lower energy, with the nucleus remaining in an excited state (inelastic channels). The excitation and decay of levels in the (γ,γ') reaction is shown in Fig. 5.

The cross section for γ inelastic scattering with isomer excitation is determined by the absorption cross section multiplied by the relative probability for a transition from the initial state to the isomeric state:

$$\sigma_m=\sigma_0\frac{b_m}{\Sigma_i b_i}, \tag{4.1}$$

where σ_0 is the absorption cross section, and b_m and b_i are, respectively, the probabilities for a transition to the isomeric state and to all the other levels.

The theory of the interaction of electromagnetic radiation with a nucleus gives an expression for the cross section for γ absorption by an individual nuclear level (the Breit–Wigner formula):

$$\sigma_0=\frac{\lambda^2}{8\pi}\frac{(2I_i+1)}{(2I_0+1)}\frac{\Gamma_i\Gamma_0}{[(E-E_0)^2+1/4\Gamma_0^2]}, \tag{4.2}$$

where λ and E are the γ wavelength and energy, Γ_0 and Γ_i are the total and partial (for a transition to the ground state) reduced widths of the excited level, E_0 is the resonance energy (the energy of the excited state), and I_0 and I_i are the spins of the ground and excited states.

Using Eqs. (4.1) and (4.2) and expressing the probabilities b_i and b_m in terms of the reduced widths, we see that in the case of a resonance $(E=E_0)$

$$\sigma_m=\frac{\lambda^2}{8\pi}\frac{2I_i+1}{2I_0+1}\cdot\frac{\Gamma_m\Gamma_i}{\Gamma_0^2}. \tag{4.3}$$

The integrated cross section of the (γ,γ') reaction includes the excitation of an entire series of levels in the energy range $E_m-E_{\gamma\,\max}$ and is expressed as

$$\sigma_{\rm int}=\int_{E_{\rm th}}^{E_{\gamma\,\max}}\sigma_m(E)dE=\sum_i\Gamma_i\sigma_m(E). \tag{4.4}$$

4.2. Statistical calculation of the isomeric ratios

Nuclear reactions occurring with the formation of a compound nucleus are usually analyzed theoretically using the statistical theory. This approach makes it possible to obtain information about the reaction mechanism, in particular, about the nuclear moment of inertia, the spin and energy dependence of the level density, and the nature of the transitions between highly excited nuclear states.

The basic element of all practical applications of the statistical theory of nuclear reactions is the level density of excited nuclei, which is commonly calculated using the expressions from the Fermi-gas model.[23] First, these expressions are fairly simple, which is an advantage in numerical calculations, and, second, they contain only three parameters: the energy parameter of the level density a, proportional to the density of single-particle states near the Fermi energy, the parameter σ^2 characterizing the dispersion of the level density in the angular momentum and proportional to the nuclear moment of inertia, and the parameter δ taking into account even–odd differences, which are usually identified with the analogous correction in the mass formula. The most direct and reliable information about the level density of excited nuclei comes from the experimental data on the density of neutron resonances. However, the various systematics of the parameters a, σ^2, and δ (Refs. 24–29) constructed on the basis of these data noticeably differ. It is therefore necessary to use data from other sources, one of which is the energy and spin dependence of the level density extracted from comparative analysis of the theoretically calculated and experimentally measured isomeric ratios.

Huizenga and Vandenbosch[5] have proposed the cascade–evaporation model based on the statistical theory for calculating the IRs as functions of the incident-particle

energy. The idea of the model is basically the following. The nucleus formed after the evaporation of one or several particles decays by a cascade of electric dipole γ quanta with fixed multiplicity equal to the average number of γ transitions. As a result of this cascade, the dispersion of the distribution of the nuclei in their spin increases. The final γ transition of the cascade (the "decisive" transition) leads to the population of one of the states of the isomeric pair. Here the competition between neutrons and γ quanta is not taken into account. Therefore, in their original formalism Huizenga and Vandenbosch used the approximate dependence of the number of emitted neutrons and γ quanta on the excitation energy. In addition, the discrete levels of the residual nuclei are neglected and it is assumed that only dipole emission occurs without competition between neutron and γ emission. This simple approach has been used to describe satisfactorily the energy dependences of the IRs from PNRs and the radiative capture of neutrons of energy $E_n<5$ MeV for a wide range of mass numbers, and also to study the effect of the level-density parameters on the IRs, the limits of applicability of the formalism, and model representations of the level density.[27–29]

Various aspects of this formalism were later improved, so that its range of applicability was extended. The competition between decay channels and the energy dependence of the spectra of evaporated particles and γ quanta were taken into account, M1, E1, and E2 transitions were included in the γ cascade, and various expressions were proposed for the reduced radiative strength functions, including ones which take into account the effect of the giant dipole resonance.

For example, in the absorption of a γ quantum of energy E_γ and multipole order $L=$E1, M1, and E2 by an even–even nucleus, initial compound states are formed with precisely determined characteristics: the energy is $E=E_\gamma$, and the spin and parity are $I^\pi=1^-$, 1^+, and 2^+. The compound nucleus deexcites by emitting a cascade of γ quanta or particles (n, p, and α). The spectrum of levels of each residual nucleus produced in the γ-capture reaction consists of two regions: the region of low-lying levels characterized by definite energy E_i and spin and parity I_i^π, and the region of levels lying above the discrete ones. These form a continuum and are described in terms of their density. This continuum of levels extends from the maximum excitation energy of the initial compound nucleus to the first known discrete level. According to this picture, there are three types of transition in a compound nucleus: (1) transitions between continuum levels; (2) transitions between continuum levels and discrete levels; (3) transitions between discrete levels. The known data from level schemes are usually used for the latter.

The population of the lower levels of the nucleus (including the isomeric levels) depends on the γ energy, the properties of the initial and final states, and the spin and energy dependence of the level density.

The cross sections for the photoabsorption of a γ quantum of energy E_γ by a target nucleus of spin and parity I_0^π with the formation of compound states in the continuum of energy E^* and spin and parity I^π is given by the expression

$$\sigma(E^*,I^\pi)=(\pi\lambda^2)g_j\frac{\Gamma_i}{D_j}, \tag{4.5}$$

where λ is the γ wavelength, g_j is the statistical factor, D_j is the average distance between levels of the compound nucleus, and Γ_i is the average partial width for a transition between the ground and compound states.

The probability for a radiative transition from the nuclear state $i(E_i^*,I_i,\pi_i)$ to the state $f(E_f^*,I_f,\pi_f)$ can be found from the expression

$$dW_{if}=\frac{\Gamma_{if}}{\Gamma_{\text{tot}}^i}\rho(E_f^*,J_f^{\pi_f})dE_f, \tag{4.6}$$

where Γ_{if} and $\Gamma_{\text{tot}}^i=\Sigma_f\Gamma_{if}$ are the partial and total widths of the level i, and $\rho(E_f^*,I_f^{\pi_f})$ is the level density of the state f.

In the region lowest in excitation energy $E^*\leqslant E_c^*$ (E^* is the excitation energy of the last known level), the nuclear levels are given on the basis of the spectroscopic data:

$$\rho(E^*,I^\pi)=\sum_{f=1}^{N}\delta(E^*-E_f^*)\,\delta_{JJ_f}\delta_{\pi\pi_f}, \tag{4.7}$$

where N is the number of known low-lying levels.

The level density of the studied nuclei for excitation energy $E^*>E_m^*$ (the maximum energy) is described by the Fermi-gas model:[26]

$$\rho(E^*,I^\pi)=f(I)\frac{\exp[2\sqrt{a(E^*-\Delta)}]}{12\sqrt{2}\sigma a^{1/4}(E^*-\Delta)^{5/4}}, \tag{4.8}$$

where a is the level-density parameter, Δ is the evaporation energy,[24]

$$f(I)=\frac{(2I+1)}{2\sigma^2}\exp\left[-\frac{(I+1/2)^2}{2\sigma^2}\right] \tag{4.9}$$

is the spin dependence of the level density, and

$$\sigma^2=(6/\pi^2)0.146A^{2/3}\sqrt{a(E^*-\Delta)} \tag{4.10}$$

is the spin-cutoff parameter.

At excitation energy $E_c^*\leqslant E^*\leqslant E_m^*$ the level density is described by the constant-temperature model:[24]

$$\rho(E^*,I^\pi)=f(I)\frac{1}{T}\exp[(E^*-E_0)/T], \tag{4.11}$$

where E_0 is a fitted parameter and T is the nuclear temperature. In this region the spin-cutoff parameter σ is determined by interpolating between the value of σ_D^2 calculated for N known low-lying nuclear levels with spins I_i,

$$\sigma_D^2=\frac{1}{2N}\sum_{i=1}^{N}(I_i+1/2)^2, \tag{4.12}$$

and the value of σ^2 from (4.10) for $E^*=E_m^*$:

$$\sigma^2(E^*)=\frac{\sigma^2(E_m^*)-\sigma_D^2}{E_m^*-E_c^*}(E^*-E_c^*)+\sigma_D^2. \tag{4.13}$$

The parameters E_m^*, T, and E_0 are chosen with the conditions that for $E^*=E_c^*$ the value of $\rho_L(E^*,I^\pi)$ found from

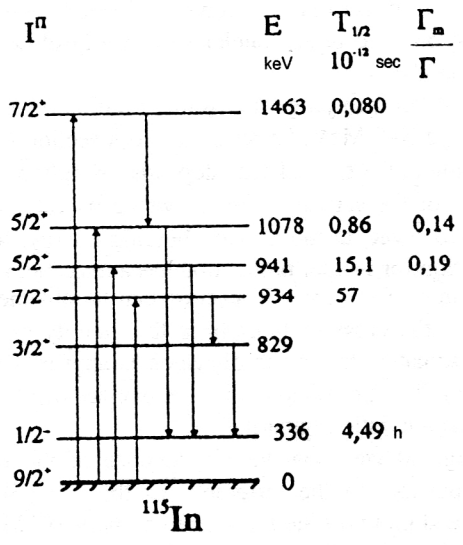

FIG. 6. Isomer population in the reaction $^{115}\mathrm{In}(\gamma,\gamma')^{115m}\mathrm{In}$.

(4.12) is equal to $\rho_L(E_c^*, I^\pi)$, and that $\rho(E)$ and $d\rho(E)/dE$ are continuous in going from Eq. (4.8) to Eq. (4.11).

4.3. Systematics of the cross sections for isomer excitation in γ inelastic scattering

The systematics of the cross sections of (γ,γ') reactions with the excitation of isomeric states includes their dependence on the γ energy and on the nucleon content of the nucleus. It is usual to distinguish three energy ranges, each with its own features:

1. The range from the energy of the isomeric level to 2 MeV.
2. The range from 2 to 6 MeV.
3. The region of the neutron binding energy (6–8 MeV).

In the first region the characteristics of the activation levels (their energies, spins, parities, lifetimes, and decay modes) are usually known. In Fig. 6 we show the scheme for isomer population in the ^{115}In nucleus via known activation levels.[30] The parameters of these levels can be used to calculate the cross sections for their excitation in γ absorption, and the probabilities for transitions from them to the isomer can be used to calculate the isomer excitation cross section. The results can then be compared with the experimental data.

Monochromatic γ sources are usually used for isomer excitation by γ quanta in this energy range (see Table I). The known experimental data on isomer excitation by γ quanta of energy below 3 MeV are summarized in Table V.[31–35] We give the characteristics of the isomeric and activation levels (their energies, spins, parities, and the probabilities of transitions to the isomer), and also the experimental integrated cross sections for the excitation of several isomers. We find good agreement between the experimental cross sections and those calculated on the basis of the known characteristics of the activation levels, which confirms the isomer-excitation mechanism considered above. When the characteristics of the activation levels are unknown, the measured cross sections of the (γ,γ') reactions with isomer population make it possible to estimate their values.

At higher excitation energies (2–6 MeV) the activation levels via which isomers are populated in the (γ,γ') reaction are, as a rule, not known from the spectroscopic data. Hints of their existence come from measurements of the dependence of the yield of nuclei in the isomeric state on the γ energy. As can be seen from Fig. 7, there are kinks in these dependences at the γ energies 2.8 MeV and 3.3 MeV in the reaction $^{115}\mathrm{In}(\gamma,\gamma')^{115m}\mathrm{In}$ (Ref. 36), and at 3 MeV and 4 MeV in the reaction $^{89}\mathrm{Y}(\gamma,\gamma')^{89m}\mathrm{Y}$ (Ref. 37). These kinks correspond to individual levels or groups of levels via which isomers in the ^{115}In and ^{89}Y nuclei are excited.

These levels also appear in the resonance scattering of γ quanta on ^{115}In and ^{89}Y nuclei. In the measured γ spectra there are prominent γ lines corresponding to radiative transitions from these levels to the ground state.[36,37] It follows from these γ spectra and isomer yields that the integrated cross sections for the excitation of these levels are considerably larger, reaching several eV·b. This is significantly larger than the cross sections for exciting individual levels at energies below 2 MeV (Table V). Another feature of isomer excitation in this energy range is the small number of activation levels with such large cross sections (altogether, 2–3 in the energy range 2–6 MeV).

Thus, at energies above 2 MeV isomer excitation in inelastic γ scattering occurs via a limited number of levels,

TABLE V. Cross sections for isomer excitation by monochromatic γ quanta.

Nucleus	I_g^π	E_m keV	I_m^π	E_a keV	I_a^π	Γ_i/Γ_0	$\sigma_{int}\cdot\Gamma_0$ b·eV		
							^{60}Co	^{24}Na	^{137}Cs
^{77}Se	$1/2^-$	168	$7/2^+$	250	$5/2^-$				0.011
				440	$5/2^-$				
				521	$3/2^-$				
^{79}Br	$3/2^-$	207	$9/2^+$	384	$5/2^+$				0.003
^{87}Sr	$9/2^+$	388	$1/2^-$	1229	$5/2^+$	0.18	0.032		
^{113}In	$9/2^+$	393	$1/2^-$	1021	$5/2^+$	0.12			
				1131	$5/2^+$	0.17	0.020		
^{115}In	$9/2^+$	335	$1/2^-$	941	$5/2^+$	0.14			
				1078	$5/2^+$	0.19	0.38	0.60	
^{176}Lu	7^-	180	1^-	~1000	6^-	0.76	0.25	110	
^{191}It	$3/2^+$	171	$1/2^-$	659	$3/2^-$				0.008

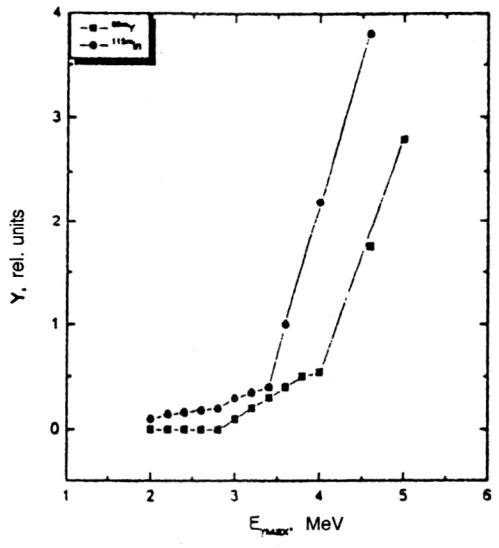

FIG. 7. Dependence of the yield of the reactions $^{115}\mathrm{In}(\gamma,\gamma')^{115m}\mathrm{In}$ and $^{89}\mathrm{Y}(\gamma,\gamma')^{89m}\mathrm{Y}$ on the maximum energy of the bremsstrahlung radiation.

which are characterized by large values of the γ-absorption cross sections.

As the excitation energy increases and the neutron binding energy is approached, the cross section for (γ,γ') reactions leading to an isomer grows noticeably. One example [the excitation function of the reaction $^{115}\mathrm{In}(\gamma,\gamma')^{115m}\mathrm{In}$] is shown in Fig. 8. The cross section grows rapidly, reaching a maximum at neutron binding energies, and then falls. This behavior of the cross section with excitation energy is apparently related to the fact that as the nucleon threshold is approached the number of levels which absorb γ quanta increases sharply, and at energies above the nucleon threshold excited states decay mainly via neutron emission.

In Fig. 9 we show the dependence of the cross sections for (γ,γ') reactions with isomer excitation on the number of neutrons in the nucleus. One of the dependences corresponds to an excitation energy of 6 MeV and is for the integrated cross sections,[38] and the other corresponds to the neutron binding energy and is for the differential cross sections.[39] We see that the two dependences are similar. The maximum

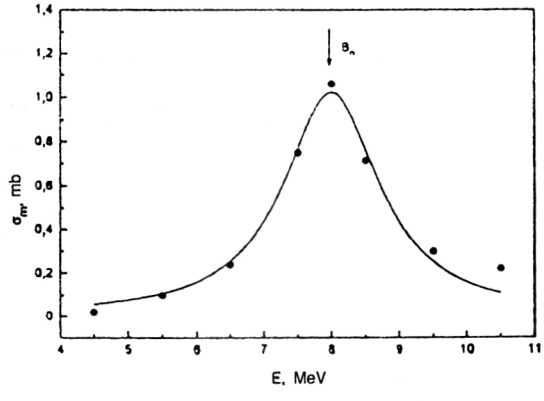

FIG. 8. Excitation function of the reaction $^{115}\mathrm{In}(\gamma,\gamma')^{115m}\mathrm{In}$ near the neutron binding energy.

cross sections occur in the region of deformed nuclei, and the minimum ones occur for nuclei with nearly closed neutron and proton shells.

It is difficult to judge the isomeric ratios for γ energies in the range 2–6 MeV, because the cross section for a reaction leading to the ground state depends strongly on the characteristics of the activation levels, which usually are poorly known. However, at the neutron binding energy, where the cross section for isomer production has a maximum, the total cross section of the (γ,γ') reaction can be obtained by extrapolating the cross sections from the vicinity of the giant dipole resonance, the shape of which is approximated by a Lorentzian. The IRs obtained in this manner display a number of characteristic regularities.

In Fig. 10 we show the dependence of the IR in the (γ,γ') reaction on the difference of the spins ΔI of the isomeric and ground state for a given γ energy (7 MeV). The largest value $\sigma^m/\sigma^g=0.47$ was observed in the case of $^{167}\mathrm{Er}$, for which $\Delta I=3$. As ΔI increases the isomeric ratio decreases sharply and reaches the value 10^{-6} for $^{190}\mathrm{Os}$, where $\Delta I=10$. At the same time, there is a large spread in the IR values; note, for example, the anomalously high value of the IR in the reactions $^{176}\mathrm{Lu}(\gamma,\gamma')^{176m}\mathrm{Lu}$ and $^{180m}\mathrm{Ta}(\gamma,\gamma')^{180}\mathrm{Ta}$ (Ref. 40).

In Fig. 11 we show the experimental values of the IRs for nuclei with $\Delta I=4$ at $E=7$ MeV as a function of the mass number A (Ref. 39). The straight line corresponds to the dependence $\sigma_m/\sigma_g=6\times10^{-4}\,A$. Thus, in this range of mass numbers the IR increases linearly with increasing mass number, and this dependence agrees well with the calculation using the statistical theory.

4.4. Excitation of high-spin isomers

It is very interesting to make a more detailed study of the behavior of the IR for (γ,γ') reactions leading to the formation of high-spin isomers in even–even nuclei. There are three types of such nuclei: strongly deformed ($^{180m}\mathrm{Hf}$), transitional ($^{190m}\mathrm{Os}$), and spherical ($^{204m}\mathrm{Pb}$).[41] It should be added that the first two nuclei ($^{180}\mathrm{Hf}$ and $^{190}\mathrm{Os}$) are typical examples of K isomers (where K is the difference in the projections of the isomeric and ground-state spins on the nuclear symmetry axis).

In Table VI we give the main characteristics of these isomers (their energy, spin, parity, multipole order of the radiative transition to low-lying states, and selection rule in the quantum number K for these transitions). We see that in the case of $^{180m}\mathrm{Hf}$, the E1 radiative transition leading to isomerism is forbidden, owing to the large change of K ($\Delta K=8$).

In the absorption of a γ quantum by an even–odd nucleus ($I=0$), the excited state will have $I^\pi=1^-$, and $K=1$ for the deformed nuclei $^{180}\mathrm{Hf}$ and $^{190}\mathrm{Os}$. Isomer population via a γ cascade is associated with a large change of both the spin I and its projection on the symmetry axis K. By comparing the IRs for deformed nuclei ($^{180}\mathrm{Hf}$ and $^{190}\mathrm{Os}$), it may be possible to judge the effect of the selection rule in the quantum number K on isomer excitation in γ inelastic scattering.

In Fig. 12 we show the dependences of the cross sections

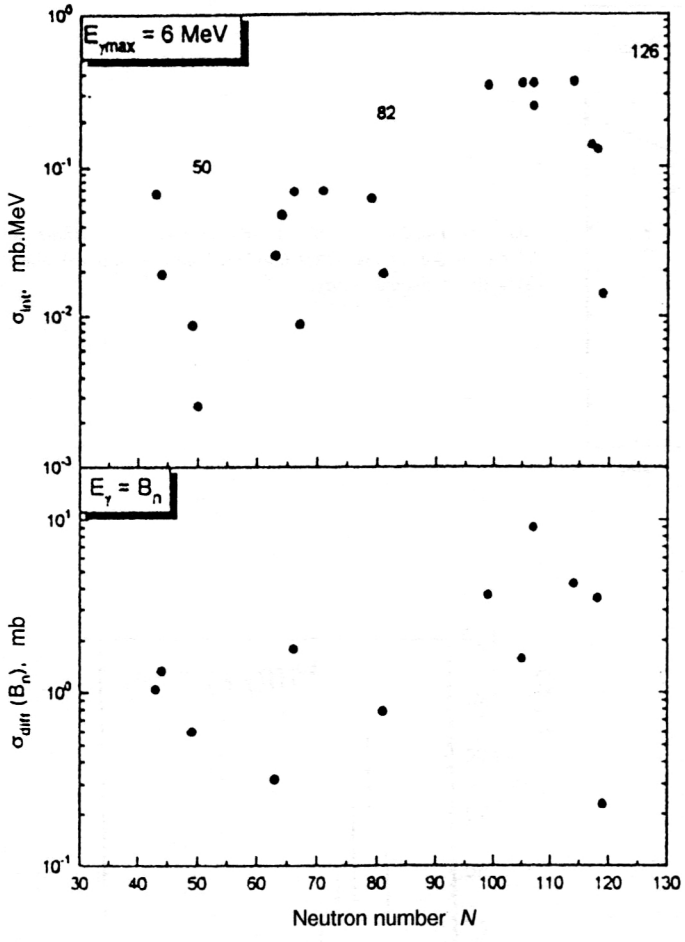

FIG. 9. Dependence of the cross sections for (γ,γ') reactions with isomer excitation on the number of neutrons in the nucleus. The integrated cross sections for $E_{\gamma_{max}}=6$ MeV are shown at the top, and the differential cross sections for $E_\gamma=B_n$ are shown at the bottom.

on the γ energy. They have a resonance shape and, within the measurement error, their maxima coincide with the threshold B_n of (γ,n) reactions. The parameters of these resonance curves are given in Table VII. The steep falloff of the cross sections for energy above B_n is related to the competition from the neutron channel ($\Gamma_n \gg \Gamma_\gamma$), which becomes important for $E_\gamma \geqslant 9$ MeV and leads to a significant decrease of the total cross section for (γ,γ') reactions. At the same time, the falloff of the cross section at lower energies is obviously related to the decrease of the number and energy of the cascade γ quanta populating the isomeric states.

In Fig. 13 we show the dependences of the IRs for these nuclei on the excitation energy. We see that the IRs are small and depend relatively weakly on the excitation energy. The

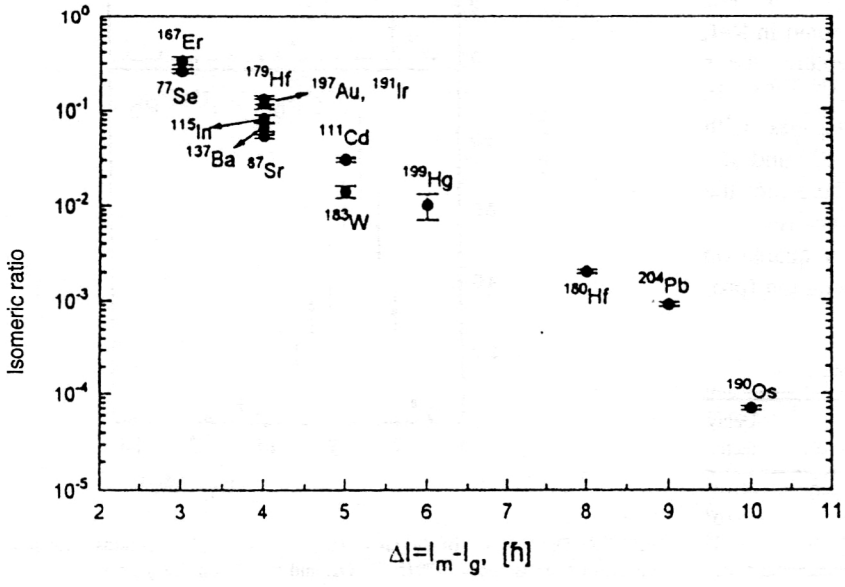

FIG. 10. Dependence of the IRs in (γ,γ') reactions on the difference of the spins of the isomeric and ground states.

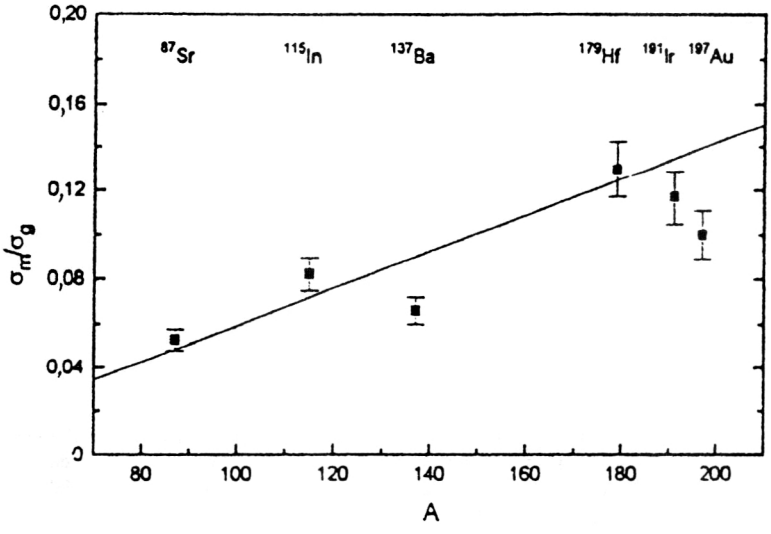

FIG. 11. Dependence of the IRs in (γ,γ') reactions for $\Delta I=4$ on the nuclear mass number. The line was calculated using the statistical theory.

closeness of the values of the IRs for the nuclei studied, including the strongly deformed nucleus ^{180}Hf and the spherical nucleus ^{204}Pb, indicates that the quantum number K weakly affects the excitation probability of high-spin isomers. Obviously, there are practically no manifestations of selection rules in the quantum number K at excitation energies where γ transitions to an isomeric level occur.

4.5. Deexcitation of the high-spin isomer ^{180m}Ta

The smaller cross sections of the three high-spin isomers discussed above contrast sharply with the isomer in the odd–odd nucleus ^{180m}Ta. This isotope of ^{180}Ta is an extremely rare nuclide. Its makes up only 0.012% of the natural mixture of isotopes. In addition, the natural form of this isotope is an isomer, because the ground state ^{180}Ta^g has a half-life of 8.1 hr, while that of the isomer is $\geqslant 1.2\times 10^{15}$ yr. The isomer has spin 9^- and excitation energy 75.3 keV, and the ground state has spin 1^+. According to the Nilsson diagram, the odd proton belongs to the $9/2^-$ [514] orbital, and the neutron to the $9/2^+$ [624] orbital, and the isomer spin is the sum of these angular momenta.

In addition to its unusual nuclear structure, ^{180}Ta has important astrophysical consequences. As was noted in Ref. 42, ^{180}Ta is not produced in slow neutron capture (the s process), which occurs on the stable isotopes $^{176-180}$Hf. In addition, since ^{180}Ta lies between stable isotopes with $A=180$ (^{180}Hf and ^{180}W), it cannot undergo β^- and β^+ decay following the fast r neutron process. Therefore, the question of how ^{180m}Ta is produced remains unanswered.

Experiments on the inelastic scattering of γ quanta on the high-spin isomer ^{180m}Ta leading to its deexcitation (pro-

TABLE VI. K-forbidden transitions in hafnium and osmium.

Nucleus	Multipole order	Energy, keV	$I_i^\pi \to I_f^\pi$	$K_i \to K_f$	Delay factor
^{180m}Hf	$E1$	58.0	$8^- \to 8^+$	$8 \to 0$	$\approx 10^{16}$
	$E3$	501.0	$8^- \to 6^+$	$8 \to 0$	$\approx 10^{9}$
^{190m}Os	$M2$	38.4	$10^- \to 8^+$	$10 \to 0$	$\approx 10^{8}$

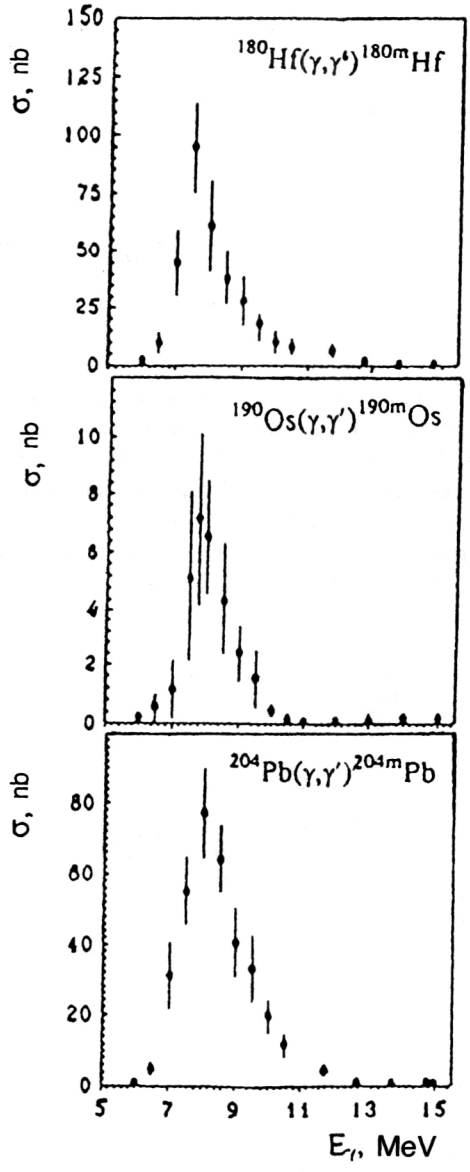

FIG. 12. Dependence of the cross sections for (γ,γ') reactions with production of the isomers ^{180m}Hf, ^{190m}Os, and ^{204m}Pb on the γ energy.

TABLE VII. Parameters of the excitation functions of the studied (γ,γ') reactions on the isotopes ^{180}Hf, ^{190}Os, and ^{204}Pb.

Reaction	E^0_{max} MeV	σ^0_{max} nb	Γ MeV
^{180}Hf(γ,γ')	7.5±0.4	95±20	1.4±0.2
^{190}Os(γ,γ')	7.9±0.5	7±3	1.2±0.4
^{204}Pb(γ,γ')	8.2±0.4	77±18	1.8±0.4

TABLE VIII. Integrated cross sections for the reactions ^{180}Hf$(\gamma,\gamma')^{180m}$Hf and ^{180m}Ta$(\gamma,\gamma')^{180}$Ta for two γ energies.

	$\sigma(\gamma,\gamma')$, mb·keV	
E_0, MeV	^{180}Hf $(0^+\to 8^-)$	^{180m}Ta$(9^-\to 1^+)$
6.5	0.015(5)	8000(3000)
7.0	0.055(10)	12000(4000)

duction of ^{180}Ta in the ground state) have shown that it has an unusually large integrated cross section.[43,44] It is 10^{-25} cm^2·keV for a γ energy of 2.8 MeV. This is the largest of all the known cross sections of (γ,γ') reactions. The cross section turned out to be just as large at the neutron binding energy.[45]

If these results are compared with inelastic scattering on ^{180}Hf, some important differences are seen. First, ^{180}Hf has an excitation scheme opposite to that of ^{180}Ta. In the case of ^{180}Hf, the isomeric level with spin 8^- and lifetime equal to 5.5 h is excited from the ground state with spin 0^+. In the case of ^{180}Ta the opposite process occurs: from the long-lived ($T_{1/2}\geq 10^{15}$ yr) isomeric state with high spin 9^- the nucleus goes to the ground state with spin 1^+ and lifetime 8.1 h. In both cases $\Delta I=8$. However, the experimental values of the cross sections differ significantly.[45] In Table VIII we give the integrated cross sections for ^{180}Hf and ^{180}Ta at two values of the γ energy.

The integrated cross sections for ^{180}Ta are four orders of magnitude higher than σ_{int} for ^{180}Hf. The large difference in the spin for ^{180}Ta apparently does not hinder its deexcitation.

As noted above, the isomeric state of ^{180}Hf decays via the single-particle states of the ground rotational band ($K=0$). The deexcitation scheme for ^{180}Ta is apparently the following (Fig. 14). States with spin and parity 8^+, 9^+, and 10^+ are excited in the dipole absorption of γ quanta from the 9^- isomeric state. These states have excitation energies of 6.5–7 MeV. The direct transition from these states to the ground 1^+ state is of low probability, owing to the large difference between the spins, $\Delta I>7$. Therefore, the M1 and E2 transitions to the ground rotational band with $K^\pi=1^+$ are more probable. The rotational levels of these bands with spins 7^+, 8^+, and 9^+ lie in the energy range 0.6–1.2 MeV. However, in this case transitions are strongly K-forbidden because $\Delta K=8$. It is known from the experimental data that in odd nuclei the level density is large even at relatively low excitation energies, and K-mixing can occur. Therefore, the forbiddenness in K is lifted and transitions from the 8^+, 9^+, and 10^+ states ($K=9$) to the 7^+, 8^+, and 9^+ states ($K=1$) become possible. Then an ordinary cascade occurs in the band, leading to the 1^+ ground state ($K=1$). Transitions from the 8^+, 9^+, and 10^+ excited states to other bands with

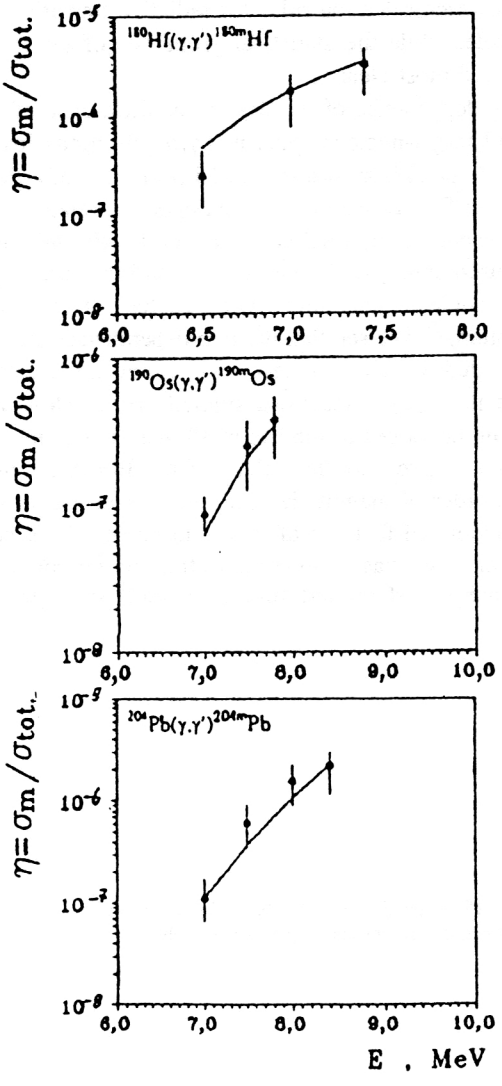

FIG. 13. Dependence of the IRs in (γ,γ') reactions with formation of high-spin isomers on the excitation energy.

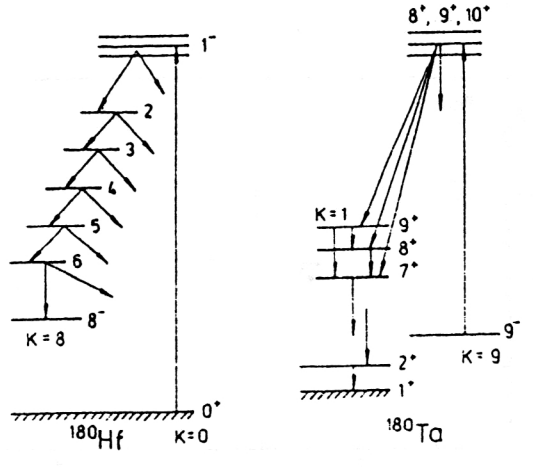

FIG. 14. Excitation scheme of the high-spin isomer ^{180m}Hf and deexcitation scheme for ^{180m}Ta.

TABLE IX. Reduced probabilities of transitions to activation levels in the isotopes ^{180}Ta and ^{115}In.

Nucleus	E_a MeV	$\sigma\Gamma$ b·eV	Γ_0 eV	B(E1) W.u.	B(M1) W.u.	B(E2) W.u.
^{180}Ta	2.8	120(20)	1.0(2)	$2\cdot10^{-2}$	2	100
	3.6	350(50)	4.8(7)	$6\cdot10^{-2}$	5	160
^{115}In	2.8	5.4(8)	0.035(5)	10^{-3}	0.07	7
	3.3	7.6(1.2)	0.10(2)	$1.2\cdot10^{-3}$	0.12	12

$K=1$, $K=3$, and $K=4$ are also possible. In the case of ^{180}Hf such a transition from a band constructed on an isomeric state is impossible, because after dipole absorption of a γ quantum there are no states with spin close to the spins of the excited states.

The known values of the level-density parameters in the vicinity of the neutron binding energy can be used to estimate the cross section for γ absorption and to find the IR for ^{180}Ta. It turns out to be 0.20(7) for $E_\gamma=6.5$ MeV and 0.25(8) for $E_\gamma=7.0$ MeV. If it is assumed that such IRs will occur at the excitation energies 2.8 MeV and 3.6 MeV, at which resonance activation levels with very large cross sections for isomer excitation are observed, then the measured cross sections can be used to find the reduced partial widths for radiative transitions from these levels to the isomer. These values of Γ are given in Table IX (the values of Γ for similar levels in ^{115}In are given for comparison).

These values of the partial widths give information about the reduced probabilities of transitions of various multipole orders (E1, M1, E2) between activation levels and the isomer. We see that for E1 and M1 transitions the values of $B(E\lambda)$ are anomalously large, which so far has not been observed. An entire group of levels may exist at these energies, so that the transition strength is distributed among a large number of levels. Meanwhile, the values of $B(E\lambda)$ are reasonable for E2 transitions and all transitions in ^{115}In.

It would be very interesting to extend the studies to other high-spin isomers which can be accumulated in neutron-capture reactions or in reactions involving heavy ions. Such experiments are being carried out using the more exotic ^{178m2}Hf target ($I^\pi_m=16^+$) (Ref. 46) with a half-life of 31 yr.

5. MEASUREMENT OF THE ISOMERIC RATIOS IN PHOTONUCLEAR REACTIONS WITH NEUTRON EMISSION

5.1. Isomer excitation in odd–odd nuclei

Isomeric states are most frequently observed in odd–odd nuclei. In these nuclei the angular momentum is formed from the spins of the two odd nucleons, a proton and a neutron. For different relative orientations of the spins (parallel and antiparallel), states with strongly differing angular momenta can arise in the nucleus, and one of these can be an isomeric state.

A significant fraction of these isomeric states can be excited in PNRs with the emission of one or several neutrons, so that they have been fairly well studied. The model of Huizenga and Vandenbosch described above can be expected to be successful at calculating the IRs in these reactions. In fact, the isomeric states have low excitation energy and the same structure as the ground states. Odd–odd nuclei are characterized by a high density of levels beginning right at the ground state (there is no energy gap). In such nuclei the isomeric and ground states are reached by a branched γ cascade in which selection rules for radiative transitions play a small role, while the statistical properties of the levels are manifested most clearly.

The dependence of the IRs on the difference of the isomer and target-nucleus spins in (γ,n) reactions leading to odd–odd nuclei is shown in Fig. 15 (Refs. 47–53). For comparison, in Fig. 16 we give the analogous dependence for the (n,γ) reaction at thermal neutron energies (in this case only the neutron spin goes to the nucleus, and the resulting compound nucleus has only two values of the angular momentum).[54] We see that the two dependences are similar. As expected, the IRs decrease with increasing ΔI, as in the case of the (γ,γ') reactions studied above. However, the spread in the values of the IRs in all these reactions is rather large: for a given ΔI the values of the IRs differ by more than an order of magnitude. This may mean that in spite of the above-noted features of odd–odd nuclei, the scheme of the lower levels has an important effect in the population of the isomeric and ground states. To understand this effect

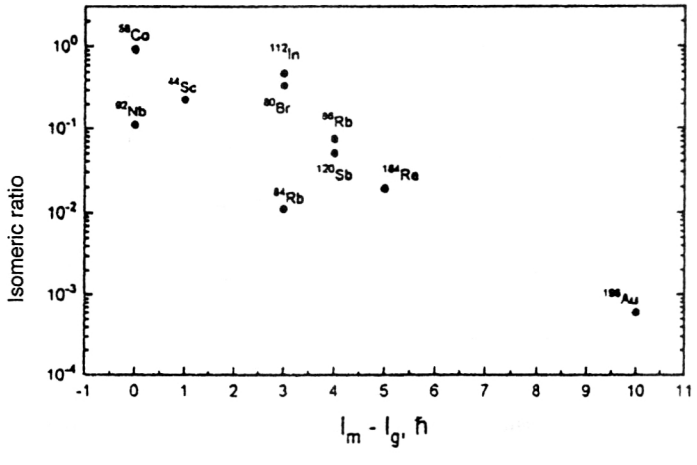

FIG. 15. Dependence of the IRs in (γ,n) reactions on the difference between the isomer and target-nucleus spins.

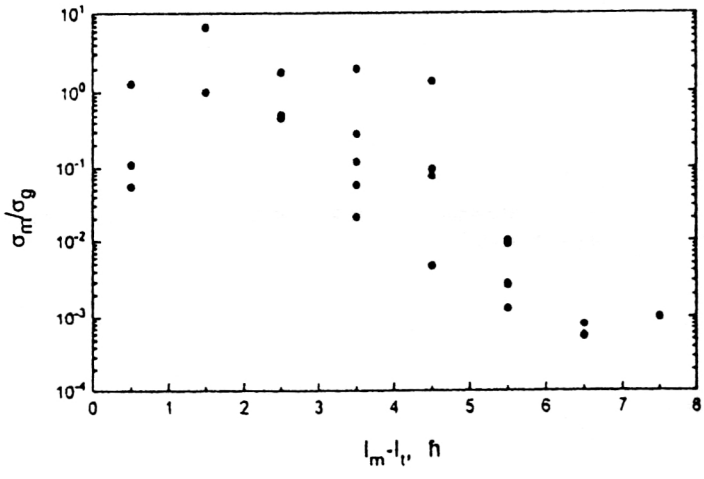

FIG. 16. The same as in Fig. 15, in (n,γ) reactions on thermal neutrons.

better, it is necessary to study reactions leading to isomeric states of the same type.

5.2. Excitation of single-particle neutron states

Detailed information about the isomer population mechanism and the properties of activation levels can be obtained by comparing the isomeric ratios in (γ,n) reactions leading to an isomer with a given nucleon configuration. Such cases are realized in (γ,n) reactions on even–even nuclei with the production of the $g_{9/2}$, $h_{11/2}$, and $i_{13/2}$ single-particle neutron states arising in the closure of shells containing 50, 82, and 126 neutrons, respectively. In particular, if the numbers Z and N lie between 30 and 49, the nuclear ground state is a $p_{1/2}$ or $g_{9/2}$ state. The second "island of isomerism" is observed for N or Z between 51 and 81, where only the $h_{11/2}$, $d_{3/2}$, and $s_{1/2}$ levels are free (or partially free). Finally, there is another when N or Z lies between 78 and 125, where the $i_{13/2}$ level can be filled.

The probability for populating these high-spin states in β decay is small, so that PNRs are convenient for studying them. The (γ,n) PNRs leading to the formation of $h_{11/2}$ isomers are the best studied.

The one-quasiparticle state with $I^\pi = 11/2^-$ arises in nuclei with $N>50$ when the $1h_{11/2}$ neutron shell is filled. By now it has been observed in more than 70 nuclei from Zr ($Z=40$) to Yb ($Z=70$).[1] In most cases (more than 50 isotopes) this state is an isomeric state with half-life greater than 1 sec, and it often can be obtained in the (γ,n) reaction.

All these isomeric states are characterized by similar values of the magnetic moments (about half the value calculated in the Schmidt model[55]) and reduced probabilities of radiative M4 transitions from the isomeric level to the $3/2^+$ state (1 to 2 Weisskopf single-particle units). This shows that the admixtures of configurations are small, and the properties of the isomeric levels are identical over the entire range of Z and A studied. It can therefore be assumed that the variations of the isomeric ratios from nucleus to nucleus will mainly be determined by the properties not of the isomers, but of the excited states via which an isomeric level is populated. The properties of these excited states differ greatly for the different nuclei studied. Among them are nuclei with a closed proton shell (Sn isotopes), nuclei with a single hole in a closed neutron shell (^{135}Xe, ^{137}Ba, ^{139}Ce, ^{141}Nd, and ^{143}Sm), and transitional nuclei between spherical and deformed ones (^{109}Pb and ^{133}Ba). In the ^{123}Sn and ^{125}Sn nuclei the $11/2^-$ state is the ground state. In the other nuclei the ground states are the $3s_{1/2}$, $2d_{3/2}$, and $2d_{5/2}$ states. The half-lives and γ energies differ considerably, and this makes it possible to make measurements simultaneously for all the nuclei studied, using samples of naturally occurring isotopic composition. Most of the isomers decay to an intermediate level via an M4 transition (they are sometimes referred to as M4 isomers). The energy of the isomeric state has a maximum at the beginning and end of the range of nuclei studied, and a minimum for $N=71-75$ in isotopes of Sn and Te.

In Ref. 56 an isomeric state was chosen with the same spin and parity $11/2^-$ for all the nuclei studied, and the isotopes involved in the reaction were even–even ones, which after absorption of a γ quantum have spin 1^-. Thus, the conditions for exciting isomeric states in all the isotopes studied were identical: the same reaction type and excitation energy, and the same spins of the initial and final states. It can therefore be expected that the changes of the experimentally measured isomeric ratios in going from one nucleus to another will be determined by how the structure of the levels via which the isomeric state is populated changes in these nuclei. The resulting experimental data can be used to understand both the statistical properties of these levels (the energy and spin dependence of their density) and their spectroscopic characteristics—their spins, parities, and probabilities of transitions of various multipole order to the isomeric state.

The measured IRs for $h_{11/2}$ states produced in (γ,n) reactions on 16 even nuclei at a maximum γ energy $E_\gamma=25$ MeV are given in Fig. 17 and Table X. We see that the IRs and also the integrated cross sections are lowest for the lightest and heaviest nuclei, which correspond to the beginning and end of the island of isomerism of these states. The Sn and Te isotopes have the maximum IRs. These measurements give information about the structure of the low-lying levels from which the last (decisive) transition to the ground or isomeric state occurs.

Tellurium nuclei are located close to the Sn nucleus with a closed proton shell and are characterized by a small change of the quadrupole deformation of these isotopes. The IR de-

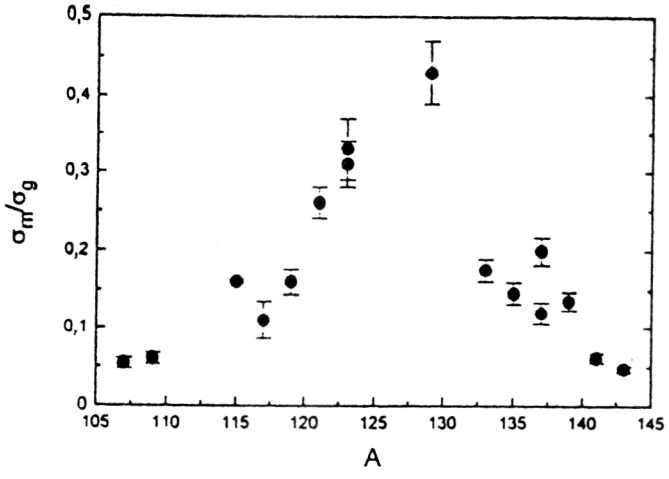

FIG. 17. Mass-number dependence of the IRs in (γ,n) reactions leading to $h_{11/2}$ states.

pendence for Te isotopes at the maximum γ energy $E_\gamma = 25$ MeV is shown in Fig. 18. The IR increases with increasing number of neutrons for Te isotopes. We see that ^{129}Te has the largest IR. This ratio also is the largest for all the $h_{11/2}$ neutron states studied. In this figure we also give the IRs for Ba isotopes at the corresponding γ energy.[57] The IR dependence has the opposite behavior for Ba isotopes: it decreases as the magic number of neutrons (^{138}Ba) is approached. This is related to the decrease of the level density in approaching the closed neutron shell $N=82$. Ba isotopes are discussed in more detail below.

There are considerably fewer data on the IRs for $g_{9/2}$ and $i_{13/2}$ neutron states.[58–62] They are given in Table XI. It should be noted that, as a rule, the $g_{9/2}$ level is the ground state, and the $s_{1/2}$ level is the isomeric state. However, in this case the IR is understood to be the ratio of the excitation cross sections for the high-spin $(9/2^+)$ and low-spin $(1/2^-)$ levels. Although the IRs given in Table XI pertain to different excitation energies and are ratios of yields rather than cross sections, they suggest the following conclusions:

1. The $g_{9/2}$ levels are characterized by large excitation probability, which grows as the closed neutron shell ($N=50$) is approached. For ^{89}Zr and ^{91}Mo nuclei ($N=49$) the probability of exciting this level is larger than that for the $s_{1/2}$ isomeric level, although its spin is close to that of the initial nucleus ($I^\pi = 0^+$). These excitation probabilities are due to the dominant contribution from semidirect processes in this region of nuclei.[63]

2. As a rule, for $i_{13/2}$ levels the values of the IR are smaller than for the $h_{11/2}$ levels discussed above, which may be due to the increased difference between the spins of the isomer and the initial nucleus. In contrast to the $g_{9/2}$ levels, the excitation probability for $i_{13/2}$ isomers decreases in approaching the closed shell $N=126$.

The large amount of experimental data on the excitation of $h_{11/2}$ isomers has made it possible to study certain regions in more detail: Ba isotopes and isotopes with $N=81$.

TABLE X. Integrated cross sections for excitation of $h_{11/2}$ isomers and isomeric ratios in (γ,n) reactions.

Reaction	E_{th}, MeV	σ_{int}, mb·MeV	$\frac{\sigma_m}{\sigma_g}$
^{108}Pd$(\gamma,n)^{107m}$Pd	9.43	67(7)	0.054(6)
^{110}Pd$(\gamma,n)^{109m}$Pd	9.00	77(8)	0.060(7)
^{116}Cd$(\gamma,n)^{115m}$Cd	8.87	199(20)	0.18(2)
^{118}Sn$(\gamma,n)^{117m}$Sn	9.69	90(18)	0.11(2)
^{124}Sn$(\gamma,n)^{123m}$Sn	8.49	285(30)	0.33(3)*
^{120}Te$(\gamma,n)^{119m}$Te	10.67	209(22)	0.20(2)
^{122}Te$(\gamma,n)^{121m}$Te	10.14	307(28)	0.26(2)
^{124}Te$(\gamma,n)^{123m}$Te	9.67	379(30)	0.31(3)
^{130}Te$(\gamma,n)^{129m}$Te	8.51	460(45)	0.45(5)
^{136}Xe$(\gamma,n)^{135m}$Xe	8.00	150(20)	0.10(2)
^{134}Ba$(\gamma,n)^{133m}$Ba	9.75	256(20)	0.17(1)
^{136}Ba$(\gamma,n)^{135m}$Ba	9.38	259(20)	0.15(1)
^{138}Ba$(\gamma,n)^{137m}$Ba	9.27	162(12)	0.12(1)
^{138}Ce$(\gamma,n)^{137m}$Ce	9.98	157(20)	0.19(2)
^{140}Ce$(\gamma,n)^{139m}$Ce	9.95	223(20)	0.14(1)
^{142}Nd$(\gamma,n)^{141m}$Nd	10.66	110(15)	0.061(10)
^{144}Sm$(\gamma,n)^{143}$Sm	11.25	91(9)	0.047(4)

*The quoted value refers to the ratio of the excitation cross sections for the $11/2^-$ ground state and the $3/2^+$ isomeric state.

5.3. Measurement of the isomeric ratios for Ba isotopes

Ba isotopes have been the object of more detailed study for several reasons.

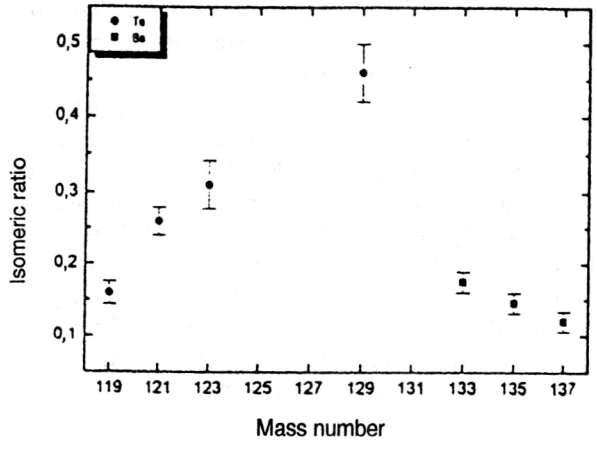

FIG. 18. Dependence of the IRs in (γ,n) reactions for Ba and Te isotopes on the number of neutrons in the nucleus.

TABLE XI. Isomeric ratios in (γ,n) reactions with excitation of $g_{9/2}$ and $i_{13/2}$ states.

Reaction	N	I_g^π	I_m^π	$E_{\gamma\max}$ MeV	$\frac{Y_{h,s}}{Y_{l,s}}$
$^{74}Se(\gamma,n)^{73m}Se$	39	$9/2^+$	$3/2^-$	22	0.86(9)
$^{86}Sr(\gamma,n)^{85m}Sr$	47	$9/2^+$	$1/2^-$	22	0.70(8)
$^{88}Sr(\gamma,n)^{87m}Sr$	49	$9/2^+$	$1/2^-$	22	0.66(16)
$^{90}Zr(\gamma,n)^{89m}Zr$	49	$9/2^+$	$1/2^-$	24	1.30
$^{92}Mo(\gamma,n)^{91m}Mo$	49	$9/2^+$	$1/2^-$	25	1.84
$^{198}Pt(\gamma,n)^{197m}Pt$	119	$1/2^-$	$13/2^+$	30	0.20
$^{196}Hg(\gamma,n)^{195m}Hg$	115	$1/2^-$	$13/2^+$	25	0.075
$^{198}Hg(\gamma,n)^{197m}Hg$	117	$1/2^-$	$13/2^+$	25	0.12
$^{208}Pb(\gamma,n)^{207m}Pb$	125	$1/2^-$	$13/2^+$	14	0.062

1. The properties of stable isotopes of barium vary strongly as the number of neutrons in the nucleus changes. The heaviest isotope ^{138}Ba has a closed neutron shell ($N=82$), and the lightest isotope ^{130}Ba is characterized by a significant quadrupole deformation ($\beta_2=0.23$). It is therefore interesting to follow how these properties affect the probability of exciting isomers in (γ,n) reactions.

2. The isomers produced in these reactions have γ spectra and half-lives convenient for measurements, which makes them easy to study.

The spectroscopic characteristics of nuclei produced in (γ,n) reactions on all the even isotopes of Ba are given in Table XII: the spins and parities of the ground and isomeric states, and the isomer energy. We see that as the nuclear deformation increases the $h_{11/2}$ levels split, and the levels with spins $9/2^-$ and $7/2^-$, respectively, become isomers in the light isotopes ^{131}Ba and ^{129}Ba.

In Fig. 19 we show the excitation functions for the isomeric states of the studied nuclei, and in Table XII we give the values of the integrated cross sections and the parameters of the giant dipole resonance: the energy E_0, the half-width Γ_0, and the cross section at the maximum, $\sigma_{\max}$, fitted by a Lorentzian.

We see from Fig. 19 that for isomeric states all these dependences have a resonance form, with resonance parameters (Table XII) close to the analogous values for the ground states. The fact that the Lorentzian curve of the isomeric states is narrower than the analogous curve for the ground states is probably related to the fact that (γ,n) channels are not distinguished from $(\gamma, 2n)$, etc., channels in experiments to measure the neutron yields.

In Fig. 20 we show the dependence of the IRs on the energy of the γ radiation (for the differential cross sections)

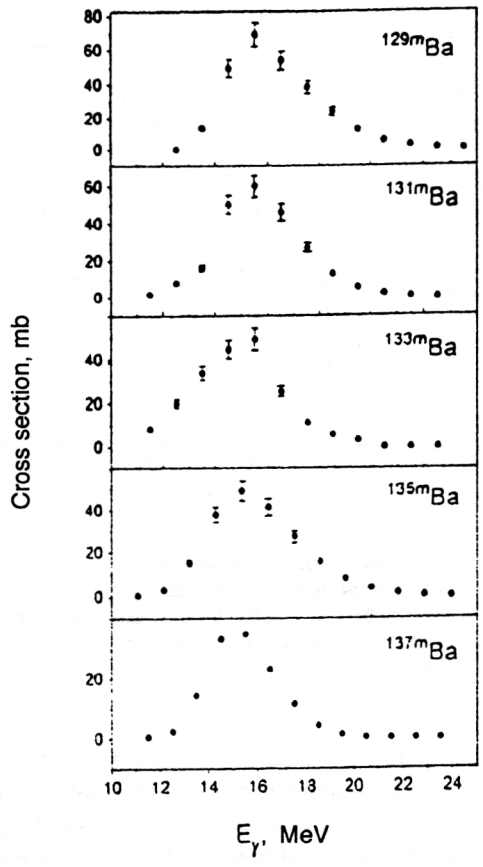

FIG. 19. Excitation functions of (γ,n) reactions leading to $h_{11/2}$ isomers in Ba isotopes.

and on the maximum energy of the bremsstrahlung radiation (for the integrated cross sections). In the latter case the IRs correspond to the ratios of the measured yields of reactions leading to the isomeric and the ground states, because the two reactions have similar excitation functions. We see from Fig. 20 that the IR varies weakly as the incident γ energy increases in the region above the giant dipole resonance. This suggests that in photonuclear reactions with the emission of a single neutron, the energy center of gravity is located in the vicinity of the giant dipole resonance (13–17 MeV). At the maximum γ energy $E_{\gamma\max}$ the average excitation energy is given by

$$\bar{E}_\gamma=\frac{\int_{E_{th}}^{E_{\gamma\max}}E\sigma(E)N(E,E_{\gamma\max})dE}{\int_{E_{th}}^{E_{\gamma\max}}\sigma(E)N(E,E_{\gamma\max})dE}, \tag{5.1}$$

TABLE XII. Characteristics of Ba isomers and parameters of the giant dipole resonance in (γ,n) reactions on Ba isotopes.

Nuclear reaction	I_g^π	I_m^π	E_m	E_0 (MeV)	Γ_0 (MeV)	$\sigma_{\max}$ (mb)	σ_{int} (MeV·mb)
$^{130}Ba(\gamma,n)^{129m}Ba$	$1/2^+$	$7/2^-$	277.0	15.3	3.1	72	347
$^{132}Ba(\gamma,n)^{131m}Ba$	$1/2^+$	$9/2^-$	187.5	15.1	2.9	64	293
$^{134}Ba(\gamma,n)^{133m}Ba$	$1/2^+$	$11/2^-$	288.3	15.1	3.1	52	256
$^{136}Ba(\gamma,n)^{135m}Ba$	$3/2^+$	$11/2^-$	268.3	15.2	3.2	52	259
$^{138}Ba(\gamma,n)^{137m}Ba$	$3/2^+$	$11/2^-$	661.6	15.2	2.6	39	162

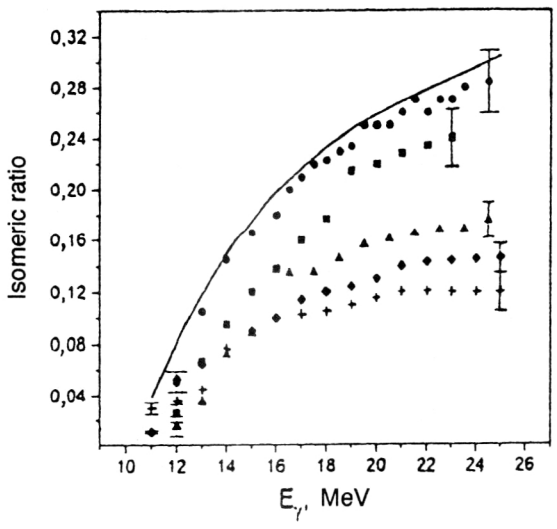

FIG. 20. Isomeric ratios for various barium isotopes in the vicinity of the giant dipole resonance (● is for ^{129m,g}Ba, ■ is for ^{131m,g}Ba, ▲ is for ^{133m,g}Ba, ◆ is for ^{135m,g}Ba, and + is for ^{137m,g}Ba), using the integrated cross sections. The solid line is the ratio of the differential cross sections for ^{129m}Ba and ^{129g}Ba.

where $\sigma(E)$ and $N(E,E_{\gamma\,\max})dE$ are, respectively, the cross section and the bremsstrahlung spectrum of the γ radiation. Calculations using this expression show that for $E_{\gamma\,\max}\geqslant 20$ MeV, E_γ corresponds to the energy of the giant dipole resonance.

As has been shown for the example of the isomer ^{137}Ce ($I^\pi = 11/2^-$), when the γ energy is increased further (up to 70 MeV), the IR hardly grows at all.[64] However, the IR is observed to grow by almost a factor of 3 if instead of the (γ,n) reaction the reaction with the emission of three neutrons is used: ^{140}Ce$(\gamma,3n)^{137m}$Ce (Ref. 65). This increase of the IR for the $(\gamma,3n)$ reaction is obviously due to the broader distribution in the nuclear angular momentum after the emission of three neutrons.

In addition, it should be borne in mind that as the maximum energy of the bremsstrahlung radiation increases (especially beyond 25 MeV), an ever greater contribution comes from direct neutron-emission processes. As is well known, these processes are especially important near magic nuclei. As noted above, they lead to a slight decrease of the isomer excitation probability with respect to the purely statistical process. Since ^{138}Ba has 82 neutrons, such pre-equilibrium processes are most noticeable in it.

The IRs in (γ,n) reactions on Ba isotopes have two features (Fig. 20).

1. The IRs grow with increasing γ energy. This growth is fairly steep below the giant dipole resonance and slower above it. Since the spin of the compound nucleus does not change (it is 1^-), the observed growth of the IRs is related to the increase of the range of excitation energy of the residual nucleus, in which a γ cascade develops.

2. The IRs grow with decreasing number of neutrons in the nucleus. The IR has a maximum for the lightest isotope ^{129}Ba. It is also correlated with the nuclear quadrupole deformation parameter. As the number of neutrons decreases and the IR grows, both the dynamical quadrupole deformation in even–even nuclei determined from the reduced E2-transition probabilities[66] and the static deformation in odd nuclei determined from the electric quadrupole moments increase.[67]

The increase of the IRs with decreasing N can be attributed to a number of factors: the spins of the isomeric and ground states, the neutron binding energies in the initial and final nuclei, the dependence of the level density of the final nucleus on the energy and spin, and the structure of the levels above the isomeric state. As can be seen from Table XII, the spins decrease in going to light isotopes of Ba. They become 1/2 for the ^{133,131,129}Ba ground states and 9/2 and 7/2 for the isomers ^{131m}Ba and ^{129m}Ba, respectively. Here the probability for populating the ground state practically does not change, because immediately above it is a level with spin 3/2 decaying only into the ground state. At the same time, the decrease of the spins of the isomeric states obviously tends to increase the IRs.

The neutron binding energy increases with decreasing N. Therefore, at γ energies corresponding to the giant dipole resonance, the excitation energy of the nucleus after neutron emission will be lower for light isotopes of Ba. This leads to a smaller energy range for the γ cascade and, accordingly, to smaller IRs. However, at large γ energies the effect of this factor will be weaker.

The level density and spin distribution of the levels in the final nucleus have an important effect on the IRs. As the parameters determining the dependence of the level density on the nuclear excitation energy and spin increase, the IR grows. Both of these parameters increase with increasing nuclear deformation, which occurs as the number of neutrons in the nucleus decreases.

Finally, the spectrum of discrete levels above the isomeric state and the probabilities for transitions between these levels determine the IRs in the final analysis. However, the data on these levels for the Ba isotopes under study are far from complete.

Calculations of the IRs using the EMPIRE program[68] based on the statistical model lead to qualitative agreement of both the measured quantities and their dependences on the excitation energy and on the number of neutrons in the nucleus. The specific values of the IRs depend on the chosen level scheme of the final nucleus.

5.4. Measurement of the isomeric ratios in isotopes with $N=81$

It is interesting to study the Z dependence of the IRs for a constant number of neutrons. The group of nuclei suitable for this consists of isotopes with closed neutron shells ($N=82$).

The reactions ^{138}Ba$(\gamma,n)^{137m,g}$Ba, ^{140}Ce$(\gamma,n)^{139m,g}$Ce, ^{142}Nd$(\gamma,n)^{141m,g}$Nd, and ^{144}Sm$(\gamma,n)^{143m,g}$Sm were studied in Ref. 56, and the isomeric ratios were found for $E_\gamma = 25$ MeV. All these nuclei have identical spins and parities in their isomeric and ground states and nearly identical quadrupole deformation coefficients in their ground states. Therefore, the IRs should not be affected by such factors as the difference between the spins of the isomeric and the ground states, which is the same for all and equal to $\Delta I = 4$. Moreover, the isomeric levels for the isotopes ^{139}Ce, ^{141}Nd, and

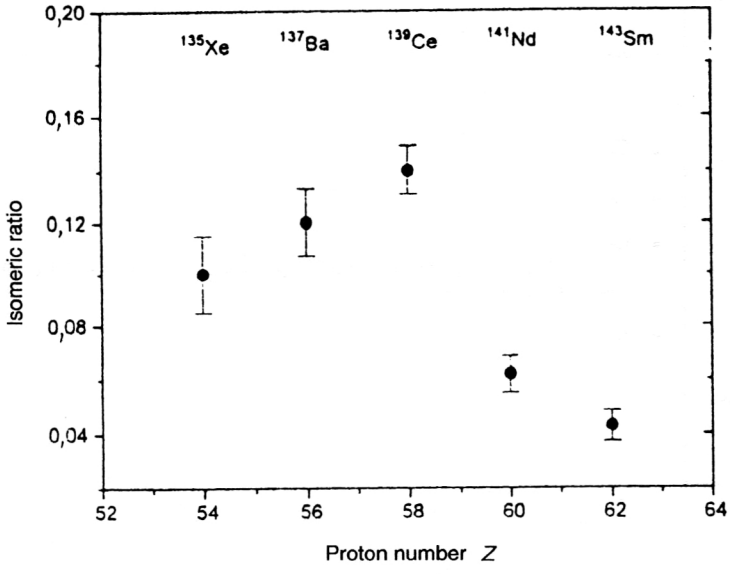

FIG. 21. Dependence of the IR in the (γ,n) reaction for nuclei with $N=81$ on the number of protons in the nucleus.

^{143}Sm have energy of order 755 keV, while for ^{137}Ba it is 661 keV. Therefore, the identical nuclear structure of the isomers implies that there should be only slight differences in their excitations.

The Z dependence of the IRs for isotopes with $N=82$ is shown in Fig. 21. The data for ^{136}Xe(γ,n) are taken from Ref. 60 for maximum γ energy equal to 22 MeV. The IR has a maximum in the vicinity of ^{140}Ce and ^{138}Ba and decreases as the closed proton shell at $Z=64$ is approached. A similar situation also apparently occurs for the left-hand side of this dependence as the other closed proton shell at $Z=50$ is approached.

The dependence of the IRs for these nuclei is exactly the same also at lower excitation energy corresponding to the maximum of the giant dipole resonance.[69] This behavior of the IRs for nuclei of similar structure is related either to a different mechanism of isomer excitation reactions, or to a different scheme of levels via which the isomers are populated.

In Ref. 69 the observed difference between the IRs was explained by assuming that pre-equilibrium processes make a large contribution (up to 70%) in isomer excitation in the ^{141}Nd and ^{143}Sm nuclei; this would tend to decrease the IRs. However, such a large contribution from pre-equilibrium processes just for these nuclei is improbable and is not consistent with the observed neutron spectrum in (γ,n) reactions.[70] The difference between the IRs seems to be mainly due to the properties of the states via which the isomers are populated.

5.5. Comparison of the experimental and calculated isomeric ratios

The above-noted similarity between the excitation functions of (γ,n) reactions leading to the isomeric and ground states suggests that these two states have the same population scheme. This scheme (Fig. 22) includes the excitation and relaxation of the giant dipole resonance, the formation of a compound nucleus, and the emission from this nucleus of a neutron and a γ cascade. Measurements of the neutron spectrum in photonuclear reactions have shown that it corresponds to evaporation from a compound nucleus with average energy $\simeq 1$ MeV (Ref. 70). At this energy the neutrons carry angular momentum $l=0$, 1, or 2 with roughly equal probability. Therefore, the sequence of spins in the isomer excitation process will be 0 (initial nucleus)$\rightarrow$1 (compound nucleus)$\rightarrow$1/2–5/2 (final nucleus)$\rightarrow$11/2 (isomer).

For this scheme the isomer excitation probability or IR can be calculated using the cascade–evaporation model discussed above.[5,68] The values of the IRs in this calculation are determined by the following factors:

1. The parameters describing the dependence of the level density on the excitation energy (a) and the angular momentum (σ). These dependences are given by Eqs. (4.8)–(4.10) and were discussed above. For the nuclei in question with

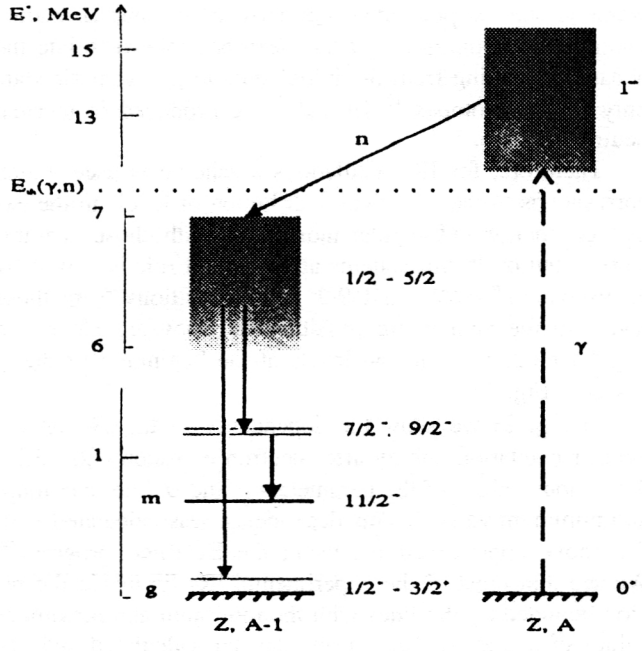

FIG. 22. Excitation of $11/2^-$ isomeric states in (γ,n) reactions.

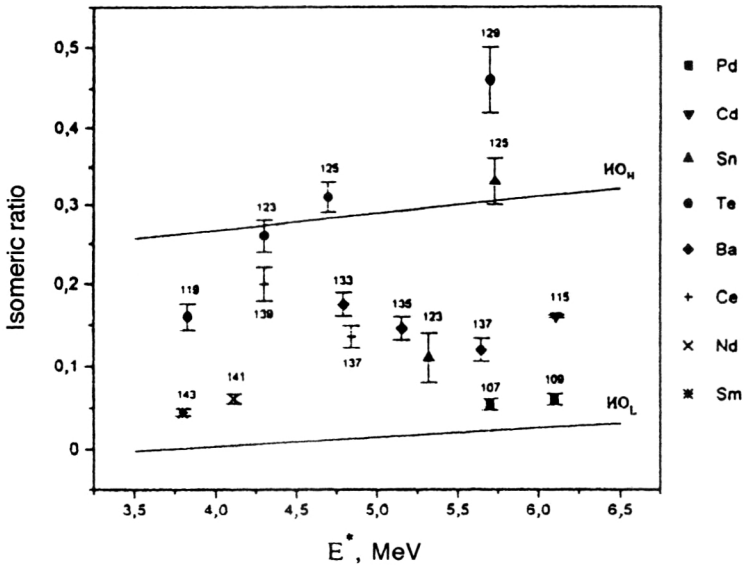

FIG. 23. Comparison of the experimental and calculated IRs for $h_{11/2}$ states.

$Z=46-62$ and $N=61-81$, the values of these parameters at the neutron binding energy are $a=11-22$ and $\sigma=3-5$ (Ref. 26).

2. The excitation energy of the nucleus after neutron evaporation and before the γ cascade. This energy is given by

$$E=\bar{E}_\gamma-B_n-\varepsilon_n, \tag{5.2}$$

where $\bar{E}_\gamma$ is the effective excitation energy after γ capture, and B_n and ε_n are the neutron binding energy and kinetic energy. It follows from the form of the excitation of (γ,n) reactions that the effective excitation energy corresponds to the location of the maximum of the giant dipole resonance and is $\simeq 15$ MeV. At this value of $\bar{E}_\gamma$ the nuclear excitation energy before the γ cascade lies in the range 3–6 MeV for different nuclei.

3. The particular scheme of levels via which the $h_{11/2}$ isomeric state is populated. For most of the nuclei studied this scheme is unknown. It has been possible to isolate the γ cascade leading from the initial state to the isomeric state only for the isotopes ^{123}Te and ^{125}Te produced in thermal neutron capture.[71]

Therefore, for IR calculations a scheme is used which corresponds to the statistical distribution of levels in the excitation energy and angular momentum with chosen parameters a and σ. In this scheme an important role is played by levels with $I^\pi=7/2^-$ and $9/2^-$. E2 transitions from these levels to the isomer are possible, and they are closest in angular momentum to the levels at the beginning of the γ cascade (Fig. 22).

In Fig. 23 we show the dependence of the IRs on the nuclear excitation energy after neutron emission [Eq. (5.2)] for various values of the parameters a and σ (the maximum and minimum values). This dependence was calculated with the above approximations, using the EMPIRE program.[68] We see that most of the experimental IRs lie inside the region bounded by the lines with the minimum and maximum values of a and σ. This means that the calculated and experimental IRs can be made to agree by choosing these parameters appropriately. However, the values of the parameters required for this can differ noticeably from those known from systematics. For example, the nearly identical values of the IRs for nuclei at the beginning and end of the island of isomerism, ^{107}Pd and ^{143}Sm, require that the values of a and σ also be close, whereas the data on neutron resonances indicate that these parameters differ significantly.

Obviously, the IRs in these nuclei are strongly affected by the properties of the levels via which isomer population occurs: their location relative to the isomers and the reduced probabilities for radiative transitions to an isomeric level. These levels are primarily $7/2^-$ and $9/2^-$ levels, and their characteristics can strongly differ for nuclei with different probabilities of exciting $h_{11/2}$ isomers.

6. EXCITATION OF SHAPE ISOMERS IN PHOTONUCLEAR REACTIONS

As noted in the Introduction, one reason for isomerism can be a great difference between the shapes of nuclei in the ground and isomeric states. This difference in shapes is usually associated with different values of the quadrupole deformation. In a number of nuclei there are known to be excited states characterized by a quadrupole deformation parameter (β_2) significantly different from that of the ground state. Three regions of such nuclei can be distinguished.

1. Transitional nuclei (on the boundary of the deformation regions), which can be weakly deformed ($\beta_2\simeq 0.1-0.2$) in isomeric states and strongly deformed in ground states ($\beta_2\simeq 0.3$), or vice versa. Examples of such nuclei are the isotopes ^{152}Eu, ^{158}Ho (in the region $N=90$), and ^{119}Cs (in the region $N=65$), in which the isomeric states have a significantly smaller deformation parameter than in the ground state.

2. Weakly deformed nuclei, in which the ground and isomeric states have deformation parameters differing not only in magnitude, but also in sign, i.e., in one of the states the nucleus is prolate, while in the other it is oblate. Ex-

amples are isotopes of Br and I near filled neutron shells and neutron-deficient isotopes of Hg.

3. Spontaneously fissioning isomers in heavy nuclei of actinide elements (from U to Bk). At present more than 40 of these are known. The characteristic feature of these isomers is the abrupt increase (by a factor of up to 10^{22}) of the probability for spontaneous fission. As a result, this decay mode dominates, which simplifies their identification and measurement. Nuclei in these isomeric states are characterized by considerably larger quadrupole deformation parameters ($\beta_2 \simeq 0.6$) than in the ground states ($\beta_2 \simeq 0.27$).

Studies of shape isomers have shown that the selection rule for γ transitions (or other deexcitation modes) determining their lifetimes depends significantly on the difference of the deformation parameters in the ground and isomeric states.[72] In the first two regions, where this difference is small ($\Delta\beta_2 \leqslant 0.15$), the forbiddenness factor is small, and it makes only an insignificant contribution to the selection rule for γ transitions, which is determined by the difference of the spins or their projections on the nuclear symmetry axis. On the contrary, in the case of spontaneously fissioning isomers, for which $\Delta\beta_2 \simeq 0.3$, the forbiddenness factor can reach $10^6 - 10^{10}$.

It is very interesting to trace how this forbiddenness factor arises in the excitation of shape isomers in various nuclear reactions. Measurements of the isomeric ratio for ^{242}Am in reactions with bombarding particles ranging from protons to heavy ions, which transfer significantly different angular momentum to the nucleus, have shown that it remains practically constant at $\simeq 4 \times 10^{-4}$ (Ref. 73). These measurements confirm the small value of the spin of spontaneously fissioning isomers and suggest that γ transitions are rather strongly forbidden in the population of the isomeric state.

These features of photonuclear reactions allow more detailed study of the shape-isomer population process and thereby a better understanding of the set of levels via which this population occurs. The (γ,γ'), (γ,n), and $(\gamma,2n)$ reactions with γ energy in the range 6–45 MeV, leading to the production of the spontaneously fissioning isomers ^{230mf}U, ^{237mf}Pu, ^{239mf}Pu, ^{241mf}Pu, ^{240mf}Am, ^{242mf}Am, and ^{243mf}Am, have been studied. The results of these studies have been systematized in Refs. 73 and 74.

In Fig. 24 we show the dependences of the yields, cross sections, and isomeric ratios on the γ energy for the (γ,n) reaction leading to the production of the spontaneously fissioning isomer ^{240mf}Am (Ref. 73). We see from this figure that the excitation function has the form typical of a reaction occurring via the formation of a compound nucleus, evaporation of a neutron from it, and then emission of a γ cascade. The isomeric ratio grows rapidly near the reaction threshold, and then emerges onto a plateau. The same form of excitation function and a similar value of the isomeric ratio ($\simeq 5 \times 10^{-4}$) also occur for other spontaneously fissioning isomers: ^{239}Pu, ^{241}Pu, and ^{242}Am (Ref. 73).

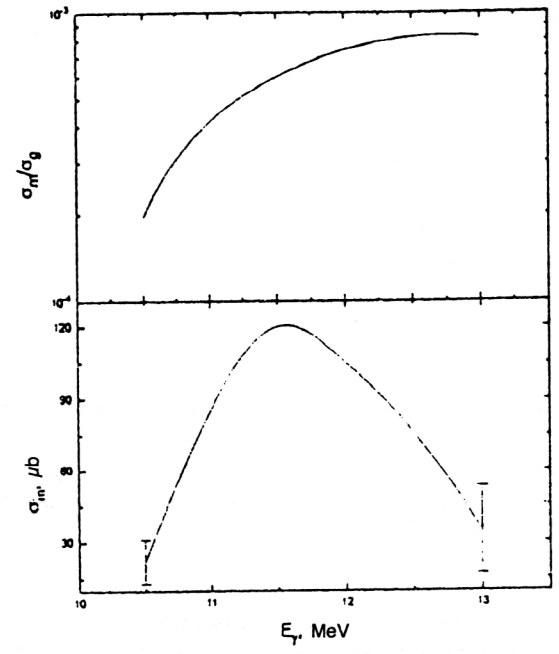

FIG. 24. Dependence of the IR and cross section for the reaction ^{241}Am$(\gamma,n)^{240mf}$Am on the γ energy.

The similar behavior of the excitation function and isomeric ratio is a reflection of a special mechanism of populating shape isomers (Fig. 25). This mechanism is a consequence of the complicated shape of the potential barrier in heavy nuclei, which has a double-humped structure and a rather deep minimum at the quadrupole deformation parameter $\beta_2 \simeq 0.6$ (Fig. 25). The lowest state of this second minimum is an isomeric state (the lowest state of the first mini-

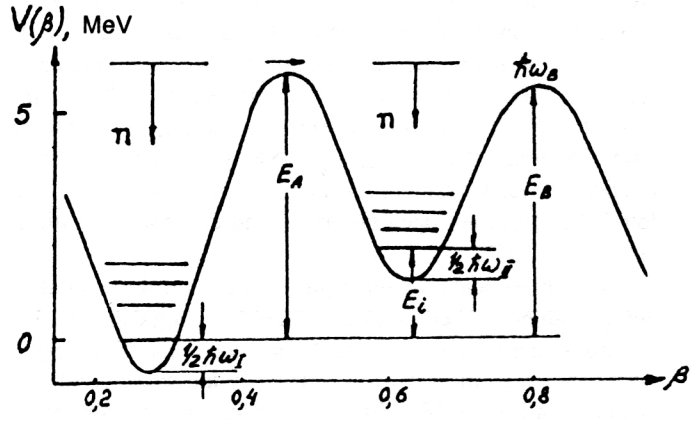

FIG. 25. Dependence of the potential energy of the nucleus on its deformation.

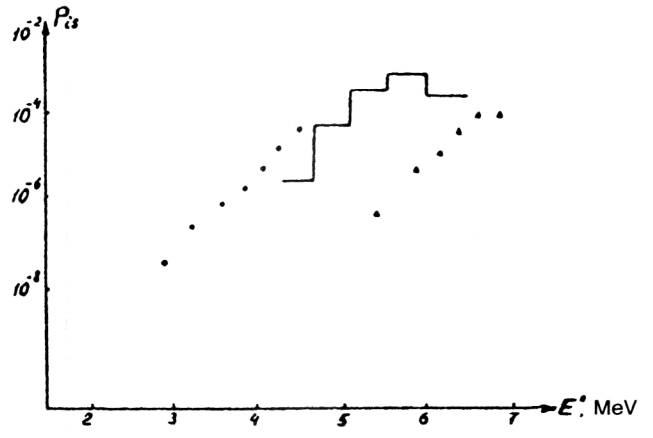

FIG. 26. Dependence of the IRs on the excitation energy in the reactions ^{235}U$(d,p)^{236m}$U (solid line), ^{238}U$(\gamma,\gamma')^{238m}$U (points), and ^{241}Am $(n,\gamma)^{242m}$Am (triangles).

mum is the ground state), and there is a whole set of levels at the second minimum. The wave functions of these levels are restricted to lie within the second well, and their overlap with the wave functions of the first well is very small. This explains why γ transitions from the isomeric level are forbidden. When it absorbs a γ quantum (or any other particle), the nucleus goes to one of the states of the first well. Owing to the strong interaction between the single-particle and collective degrees of freedom in the nucleus, part of the excitation energy can be transformed into quadrupole oscillations, and the nucleus can acquire a deformation corresponding to the second well. Here the reverse process can occur: the deformation energy can be transformed into thermal energy, and a compound nucleus with large deformation and excitation energy measured from the second well can be formed. If this is accompanied by evaporation of a neutron from the nucleus, the nucleus ends up in one of the lower states of the second well. Owing to the small overlap of the wave functions of the levels of the first and second wells, deexcitation of the levels of the second well by a γ cascade leads to the isomer. For this reaction mechanism the cross section for forming a spontaneously fissioning isomer in the (γ,n) reaction has the form

$$\sigma_m=\sigma_0\frac{\Gamma_{f1}}{\Gamma_{f1}+\Gamma_{n1}}\cdot\frac{\Gamma_{n2}}{\Gamma_{f2}+\Gamma_{n2}}, \tag{6.1}$$

where σ_0 is the cross section for compound-nucleus formation in the absorption of a γ quantum, Γ_f and Γ_n are the fission and neutron widths, and the subscripts 1 and 2 refer to the first and second potential wells. In this mechanism of populating the shape isomer the isomeric ratio is given by

$$\frac{\sigma_m}{\sigma_g}=\frac{\Gamma_{f1}}{\Gamma_{n1}}\cdot\frac{\Gamma_{n2}}{\Gamma_{f2}+\Gamma_{n2}}. \tag{6.2}$$

The characteristic feature of nuclei located in the second well is the fact that for them the barrier height E_B is significantly lower than the neutron binding energy (Fig. 26). For the studied isotopes of Pu and Am this difference is $B_n-E_B\simeq 3$ MeV. For this relation between B_n and E_B the fission width of the levels in the second well is much larger than the neutron width (this is what increases the fission probability for the second well). In this case ($\Gamma_{f2}\gg\Gamma_{n2}$) the isomeric ratio can be written as

$$\frac{\sigma_m}{\sigma_g}=\frac{\Gamma_{f1}}{\Gamma_{f2}}\frac{\Gamma_{n2}}{\Gamma_{n1}}. \tag{6.3}$$

In the statistical theory of the nucleus the neutron and fission widths at excitation energy E are given by

$$\Gamma_n=\frac{\int_0^{E-B_n}\rho(E-B_n)E_n dE}{2\pi\rho(E)}, \tag{6.4}$$

$$\Gamma_f=\frac{\int_0^{E-B_f}\rho(E-B_f)dE}{2\pi\rho(E)}. \tag{6.5}$$

If the expression obtained in the constant-temperature model is used for the level density, the isomeric ratio takes the form

$$\frac{\sigma_m}{\sigma_g}=e^{\frac{E_B-E_A-E_m}{T}}, \tag{6.6}$$

where E_A and E_B are the inner and outer fission barriers, and E_m is the energy of the isomeric level (Fig. 25). We see from Eq. (6.6) that the IR and its dependence on the excitation energy depend on the parameters of the fission barrier E_A, E_B, and E_m. Therefore, measurements of the excitation functions of reactions leading to spontaneously fissioning isomers can be used to determine these parameters. The values of the parameters of the double-humped fission barrier for Pu and Am isotopes obtained in this manner are given in Table XIII.

TABLE XIII. Fission-barrier parameters obtained from analysis of (γ,n) and (γ,γ') reactions.

Nucleus	Reaction	Barrier parameters, MeV				
		E_A	E_B	E_m	$\hbar\omega_A$	$\hbar\omega_B$
^{238}U	^{238}U(γ,γ')	6.0(3)	6.0(3)	3.0(4)	1.2(2)	0.7(2)
^{239}Pu	^{240}Pu(γ,n)		5.8(2)	3.3(3)		
	^{239}Pu(γ,γ')	6.5(3)	5.5(3)		1.0(3)	0.5(2)
^{241}Pu	^{242}Pu(γ,n)	6.1(3)	5.1(2)	2.7(3)	1.1(3)	0.6(2)
^{240}Am	^{241}Am(γ,n)	6.4(3)	5.2(2)	3.0(3)	0.7(3)	0.4(1)
^{242}Am	^{243}Am(γ,n)	6.4(3)	5.1(2)	2.4(3)	0.6(2)	0.4(1)
^{243}Am	^{243}Am(γ,γ')	6.0(3)	5.5(3)		0.7(2)	0.5(2)

Like other isomeric states, shape isomers can also be excited in the inelastic scattering of low-energy γ quanta. However, there is much less information on this type of reaction than on the (γ,n) reaction leading to spontaneously fissioning isomers. The only available data are on the cross sections for the reactions ^{239}Pu$(\gamma,\gamma')^{239mf}$Pu and ^{243}Am$(\gamma,\gamma')^{243mf}$Am for γ energies in the range 7–12 MeV (Ref. 75) [$\sigma_m\simeq 8$ μb, $(\sigma_m/\sigma_g)\simeq 5\times10^{-4}$]. The formation of spontaneously fissioning isomers at excitation energies below 7 MeV has not been observed, and the isomeric ratio is $(\sigma_m/\sigma_g)<10^{-4}$.

The dependence of the isomeric ratio on the excitation energy can be studied in greater detail by using data on other reactions, namely, (n,γ) and (d,p) reactions. The dependence for the isomers of ^{236}U and ^{242}Am including these data is shown in Fig. 26 (Ref. 76). We see that the probability for

producing spontaneously fissioning isomers falls off rapidly as the excitation energy decreases below 6.5 MeV. This excitation energy corresponds to the height of the barrier separating the two potential wells. It can be concluded from the energy dependence of σ_m/σ_g shown in Fig. 24 that the existence of this barrier makes γ transitions populating the isomeric state strongly forbidden. This forbiddenness is due to the above-mentioned small overlap of the wave functions of the excited levels of the first and second potential wells. At excitation energies above the barrier the degree of overlap of the wave functions increases, the forbiddenness of γ transitions decreases, and the isomeric ratio becomes the same as in (γ,n) reactions far from the reaction threshold.

7. CONCLUSION

By studying photonuclear reactions with the excitation of isomeric states it is possible to obtain a great deal of new data about the properties of the levels via which isomer population occurs. These data give information about the parameters of these levels: their energies, spins, parities, and nucleon configurations, and also about the multipole orders and reduced probabilities of radiative transitions between these levels and the ground or isomeric state.

At low excitation energies (below 2 MeV), the isomer is populated via levels with spin intermediate between the spins of the ground state and the isomer. These levels are connected both to the ground state and to the isomer by radiative transitions of low multipole order (E1, M1, and E2), for which the reduced transition probabilities have values typical of transitions between low-lying nuclear levels (1–10 Weisskopf units for E2 transitions, 10^{-2} W.u. and 10^{-4} W.u. for M1 and E1 transitions, respectively).

At higher energies (2–5 MeV), there are relatively few levels (or groups of closely spaced levels) involved in this excitation. These levels are connected to the ground state by radiative transitions with large reduced probabilities (10–100 times larger than for transitions between low-lying levels). Finally, in the vicinity of the neutron binding energy the nucleus upon absorbing a γ quantum ends up in any of the excited states connected with the ground state by E1 or M1 transitions.

There are two special features of isomer population from excited states:

1. For deformed nuclei, there is practically no selection rule in the quantum number K in the radiative transitions of the γ cascade leading to the isomer. Therefore, the levels of the rotational band constructed on the isomer are populated, which can significantly increase the isomer excitation probability.

2. At the same time, radiative transitions are rather strongly forbidden in the case of isomers with deformation markedly different from that of the ground state. This forbiddenness is strongest at low energies of the levels involved in isomer population and decreases as their energy increases.

[1] E. Browne and R. B. Firestone, in *Table of Radioactive Isotopes*, edited by V. S. Shiley (Wiley, New York, 1986).
[2] S. M. Polikanov, *Shape Isomerism of Nuclei* [in Russian] (Atomizdat, Moscow, 1977).
[3] E. G. Fuller and E. Hayward, in *Nuclear Reactions* [in Russian], Vol. 2, p. 114 (Atomizdat, Moscow, 1977).
[4] B. S. Ishkhanov and I. M. Kapitonov, *Interaction of Electromagnetic Radiation with Nuclei* [in Russian] (Moscow State University Press, Moscow, 1979).
[5] J. R. Huizenga and R. Vandenbosch, Phys. Rev. **120**, 1305 (1960).
[6] K. Debertin and R. G. Helmer, *Gamma- and X-Ray Spectrometry With Semiconductor Detectors* (North-Holland, Amsterdam, 1988).
[7] S. P. Kapitsa and V. M. Melekhin, *The Microtron* [in Russian] (Nauka, Moscow, 1969).
[8] L. Schiff, Phys. Rev. **83**, 52 (1951).
[9] H. Ferdinand *et al.*, Nucl. Instrum. Methods **91**, 135 (1971).
[10] Ph. G. Kondev, A. P. Tonchev, Kh. G. Khristov, and V. E. Zhuchko, Nucl. Instrum. Methods B **71**, 126 (1992).
[11] V. E. Zhuchko and Zen Chen Uk, At. Énerg. **59**, 65 (1985) [Sov. J. At. Energy].
[12] M. Z. Tarasko, A. S. Soldatov, and V. E. Rudnikov, At. Énerg. **60**, 290 (1985) [Sov. J. At. Energy].
[13] W. J. Varhue and T. G. Williamson, Appl. Radiat. Isot. **37**, 155 (1986).
[14] S. Fultz, R. L. Bramblett, J. Caldwell, and R. Harvey, Phys. Rev. **134**, B1149 (1964).
[15] S. S. Dietrich and B. L. Berman, At. Data Nucl. Data Tables **38**, 199 (1988).
[16] E. Bramanis, T. K. Deague, R. S. Hicks *et al.*, Nucl. Instrum. Methods **100**, 59 (1972).
[17] B. C. Cook, Nucl. Instrum. Methods **24**, 256 (1963).
[18] V. G. Ivanchenko, Proc. of the Lebedev Institute **63**, 151 (1972).
[19] A. S. Penfold and J. E. Leis, Phys. Rev. **114**, 1332 (1959).
[20] A. G. Tikhonov, Dokl. Akad. Nauk SSSR **151**, 3 (1963).
[21] M. Z. Tarasko, Preprint No. 156, Physics and Power Engineering Institute, Obninsk (1969) [in Russian].
[22] V. E. Zhuchko, Yad. Fiz. **25**, 299 (1977) [Sov. J. Nucl. Phys. **25**, 161 (1977)].
[23] J. M. Blatt and V. F. Weisskopf, *Theoretical Nuclear Physics* (Wiley, New York, 1952) [Russ. transl., IL, Moscow, 1954].
[24] A. V. Malyshev, *Level Density and Structure of Nuclei* [in Russian] (Atomizdat, Moscow, 1969).
[25] H. Baba, Nucl. Phys. **159**, 625 (1970).
[26] W. Dilg, W. Schant, H. Vonach, and M. Uhl, Nucl. Phys. **A217**, 269 (1973).
[27] M. L. Sehgal, Phys. Rev. **128**, 761 (1962).
[28] W. P. Pönitz, Z. Phys. **197**, 262 (1966).
[29] A. V. Ignatyuk, G. N. Smirenkin, and A. S. Tishin, Yad. Fiz. **21**, 485 (1975) [Sov. J. Nucl. Phys. **21**, 255 (1975)].
[30] C. B. Collins, J. A. Anderson, Y. Paiss *et al.*, Phys. Rev. C **38**, 1852 (1988).
[31] A. Veres and I. Pavlicsek, Acta Phys. Hung. **28**, 419 (1970).
[32] É. A. Zaparov, Yu. N. Koblik, B. S. Mazitov, and T. A. Tadyuk, *Direct Reactions and Isomeric Transitions* [in Russian] (FAN, Tashkent, 1973).
[33] Y. Watanabe and T. Mikoyama, Nucl. Sci. Eng. **80**, 92 (1982).
[34] E. B. Norman, S. E. Kellog, T. Bertram *et al.*, Astrophys. J. **281**, 360 (1984).
[35] N. X. Khan, L. Lakosi, and I. Pavlicsek, Phys. Rev. C **51**, 1676 (1995).
[36] P. von Neumann-Cosel, A. Richter, C. Spieler *et al.*, Phys. Lett. **266B**, 9 (1991).
[37] M. Huber, P. von Neumann-Cosel, A. Richter *et al.*, Nucl. Phys. **A559**, 253 (1993).
[38] J. J. Carrol, M. J. Byrd, D. G. Richmond *et al.*, Phys. Rev. C **43**, 1238 (1991).
[39] V. M. Mazur, I. V. Sokolyuk, Z. M. Bigan, and I. Yu. Kibkalo, Yad. Fiz. **56**, No. 1, 20 (1993) [Phys. At. Nucl. **56**, 10 (1993)].
[40] L. Lakosi, I. Pavlicsek, and A. Veres, Acta Phys. Hung. **69**, 169 (1991).
[41] N. P. Balabanov, A. G. Belov, Yu. P. Gangrsky *et al.*, Preprint E15-93-370, JINR, Dubna (1993).
[42] J. J. Carrol, J. A. Anderson, J. W. Glesener *et al.*, Astron. J. **344**, 454 (1989).
[43] C. B. Collins, J. W. Eberhard, J. W. Gleser, and J. A. Anderson, Phys. Rev. C **37**, 2267 (1988).
[44] C. B. Collins, J. J. Carroll, T. W. Sinoz, M. J. Byrd *et al.*, Phys. Rev. C **42**, R1813 (1990).
[45] A. G. Belov, Yu. P. Gangrskiĭ, P. Zuzaan, and A. N. Tonchev, Izv. Russ. Akad. Sci. Ser. Fiz. **60**, No. 1, 199 (1996) [Bull. Russ. Acad. Sci., Phys. Ser.].
[46] Yu. Ts. Oganessian, S. A. Karamian, Yu. P. Gangrski *et al.*, J. Phys. G **18**, 393 (1992).
[47] I. N. Vishnevskiĭ, V. A. Zheltonozhskiĭ, V. M. Mazur, and S. V.

Reshit'ko, Izv. Akad. Nauk SSSR, Ser. Fiz. **53**, 171 (1983) [Bull. Acad. Sci. USSR, Phys. Ser.].
[48] L. Z. Dzhilavyan, L. E. Lazareva, V. N. Ponamarev, and A. A. Sorokin, Yad. Fiz. **33**, 591 (1981) [Sov. J. Nucl. Phys. **33**, 308 (1981)].
[49] I. V. Bodrov, M. G. Davydov, and A. P. Mikheev, At. Énerg. **75**, 75 (1993) [Sov. J. At. Energy].
[50] V. A. Zheltonozhskiĭ, V. I. Lomonosov, V. M. Mazur, and I. V. Sokolyuk, At. Énerg. **68**, 441 (1990) [Sov. J. At. Energy].
[51] M. G. Davydov, V. G. Magera, A. V. Trukhov, and É. M. Shomurazov, At. Énerg. **58**, 47 (1985) [Sov. J. At. Energy].
[52] I. N. Vishnevskiĭ, V. A. Zheltonozhskiĭ, V. M. Mazur, and Z. M. Bigan, Vopr. At. Nauk. Tekh., Ser. Fiz. **1**, 21 (1991) [in Russian].
[53] H. Bartsch, K. Huber, U. Kneissl, and H. Krieger, Nucl. Phys. **A256**, 243 (1976).
[54] E. Gryntakis, D. E. Cullen, and G. Mundy, *Handbook on Nuclear Activation Data*, No. 273 (IAEA, Vienna, 1987).
[55] T. Schmidt, Z. Phys. **106**, 358 (1937).
[56] A. G. Belov, Yu. P. Gangrskiĭ, A. P. Tonchev, and N. P. Balabanov, Yad. Fiz. **59**, 585 (1996) [Phys. At. Nucl. **59**, 553 (1996)].
[57] A. G. Belov, Yu. P. Gangrskiĭ, A. P. Tonchev *et al.*, Yad. Fiz. **59**, 389 (1996) [Phys. At. Nucl. **59**, 367 (1996)].
[58] F. Z. Khien, N. K. Zui, and N. T. An', Yad. Fiz. **35**, 257 (1982) [Sov. J. Nucl. Phys. **35**, 145 (1982)].
[59] H. D. Luc and T. D. Thiep, Bulg. J. Phys. **14**, 153 (1987).
[60] M. G. Davydov, V. G. Magera, and A. V. Trukhov, At. Énerg. **62**, 236 (1987) [Sov. J. At. Energy].
[61] I. V. Bodrov, M. G. Davydov, I. B. Rakhmanov, and A. V. Trukhov, Yad. Fiz. **57**, 1347 (1994) [Phys. At. Nucl. **57**, 1277 (1994)].
[62] V. M. Mazur, Z. M. Bigan, and I. V. Sokolyuk, Laser Phys. **5**, 273 (1995).
[63] Z. M. Bigan, V. M. Mazur, I. V. Sokolyuk, and V. I. Lomonosov, Ukr. Fiz. Zh. **35**, No. 2, 173 (1990) [in Russian].
[64] A. G. Belov, Yu. P. Gangrsky, F. G. Kondev *et al.*, in *Proc. of the Workshop on Applications of Microtrons in Nuclear Physics*, Plovdiv, 1992, p. 106.
[65] P. E. Haustein and A. F. Voigt, J. Inorg. Nucl. Chem. **33**, 289 (1971).
[66] S. Raman *et al.*, At. Data Nucl. Data Tables **42**, 1 (1989).
[67] P. Raghavan, At. Data Nucl. Data Tables **42**, 189 (1989).
[68] M. Herman, A. Marcinkowski, and K. Stankiewicz, Comput. Phys. Commun. **33**, 373 (1984).
[69] V. M. Mazur, V. A. Zheltonozhskiĭ, and Z. M. Bigan, Yad. Fiz. **58**, 970 (1995) [Phys. At. Nucl. **58**, 898 (1995)].
[70] A. M. Goryachov and G. N. Zalesnyĭ, Izv. Akad. Nauk SSSR, Ser. Fiz. **54**, 2240 (1990) [Bull. Acad. Sci. USSR, Phys. Ser.].
[71] J. Honzatko, K. Konecny, and I. Tomandl, Z. Phys. A **345**, 429 (1993).
[72] Yu. P. Gangrskiĭ, Fiz. Élem. Chastits At. Yadra **9**, 383 (1978) [Sov. J. Part. Nucl. **9**, 158 (1978)].
[73] Yu. P. Gangrsky, B. N. Markov, and Y. M. Tsypenyuk, Fortschr. Phys. **22**, 199 (1974).
[74] U. Kneissl, W. Gunter, K. Huber, and H. Krieger, Fortschr. Phys. **30**, 311 (1982).
[75] Yu. P. Gangrskiĭ, B. N. Markov, Kh. F. Kharisov, and Yu. M. Tsipenyuk, Pis'ma Zh. Éksp. Teor. Fiz. **14**, 370 (1971) [JETP Lett. **14**, 249 (1971)].
[76] Yu. P. Gangrskiĭ, Izv. Akad. Nauk SSSR, Ser. Fiz. **41**, 920 (1978) [Bull. Acad. Sci. USSR, Phys. Ser.].

Translated by Patricia A. Millard